

**DEVELOPMENT OF LAMINATION PROCESS
TO FABRICATE OPTICAL
TRANSPARENCIES OF HURKUS-C
AIRCRAFT**



By

Safa Shahid

Muhammad Sameer

Muhammad Bilal Tariq

**School of Chemical and Materials Engineering (SCME)
National University of Sciences and Technology (NUST)**

2024

DEVELOPMENT OF LAMINATION PROCESS TO FABRICATE OPTICAL TRANSPARENCIES OF HURKUS-C AIRCRAFT



By

Leader - 335337 Safa Shahid

Member-1 - 342736 Muhammad Sameer

Member-2 - 338221 Muhammad Bilal Tariq

A THESIS

Submitted to

National University of Sciences and Technology

in partial fulfilment of the requirements for the degree of

B.E. METALLURGY AND MATERIALS ENGINEERING

School of Chemical and Materials Engineering (SCME)

National University of Sciences and Technology (NUST)

June 2024

CERTIFICATE

This is to certify that work in this thesis has been completed by **Miss Safa Shahid, Mr. Muhammad Sameer** and **Mr. Muhammad Bilal Tariq** under the supervision of **Dr. Nabeel Ahmed** and **Dr. Muhammad Irfan** at the school of Chemical and Materials Engineering (SCME), National University of Science and Technology, H-12, Islamabad, Pakistan.



Advisor:

Dr. Nabeel Ahmed

Department of Materials Engineering
School of Chemical and Materials
Engineering
National University of Sciences and
Technology

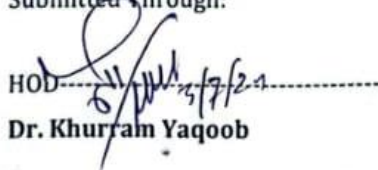


Co-Advisor

Dr Ing Muhammad Irfan

Department of Chemical Engineering
School of Chemical and Materials
Engineering
National University of Sciences and
Technology

Submitted Through:



HOD -----

Dr. Khurram Yaqoob

Department of Materials Engineering
School of Chemical and Materials
Engineering
National University of Sciences and
Technology



Principal -----

Dr. Umair Manzoor

Department of Materials Engineering
School of Chemical and Materials
Engineering
National University of Sciences and
Technology

ABSTRACT

Optical transparencies allow light to easily pass through and are widely used in applications such as lenses and optics, windows and glass panes, photovoltaic devices, displays and screens. This study aims to work on the canopy of Hurkus-C aircraft, owned by Turkish Aerospace Industries (TAI). Currently, Aircraft Rebuild Factory (ARF), located in Pakistan Aeronautical Complex (PAC), Kamra is manufacturing monolithic canopies which are made up of Polymethyl methacrylate (PMMA) or acrylic only. These canopies depict poor impact toughness. Our final year design project (FYDP) is composed on developing a lamination process of this canopy by bonding two sheets of PMMA together by using Polyurethane (PU) as an adhesive. This is placed in a hot press and heated above the melting point of polyurethane (PU) to form a strong bond between two sheets of PMMA. This will improve the impact toughness of a canopy, whose role is to provide a clear view to the pilot and protection from elements including bird strike, without affecting its optical transparencies. To check the surface morphology of our material and whether it has a smooth surface without any scratches, Scanning Electron Microscopy (SEM) analysis was performed. The surface chemistry was viewed through a technique, named Fourier Transform Infrared Spectroscopy (FTIR), which allowed us to see the chemical bonds present in PMMA and PU. The outstanding results achieved an optical transparency of more than 95%. Characterization of the laminates was conducted through tensile test, and the highest value of tensile strength was found to be 61.1 N/mm².

DEDICATION

With deep respect,

We dedicate this endeavor to our beloved parents, respected instructors, and lab engineers,
whose leadership and unwavering support encouraged us during the entire project.

ACKNOWLEDGEMENTS

We are really grateful to Allah, the Most Gracious, for enabling us to do exceptionally well on our final year design project. We sincerely thank our supervisor, Dr. Nabeel Ahmed, for his unwavering support and direction, which were crucial to the project's successful completion. We could not have accomplished this difficult task to the best of our abilities without his commitment. We also thank our co-supervisor, Dr. Ing Muhammad Irfan, whose insightful recommendations substantially advanced our comprehension and problem-solving abilities. We also appreciate the lab engineers, attendants, and research students for helping us become familiar with the equipment and processes that are necessary for our project. We would like to sincerely thank all of the Materials Engineering department's instructors and staff for their consistent support and direction during this journey.

TABLE OF CONTENTS

CHAPTER 1	0
INTRODUCTION	0
1.1 Background	0
1.2 Objectives.....	1
CHAPTER 2	2
LITERATURE REVIEW	2
2.1 Material.....	3
CHAPTER 3	4
EXPERIMENTAL WORK	4
3.1 Characterizations	4
3.1.1 Scanning Electron Microscopy (SEM).....	4
3.1.2 Atomic Force Microscopy (AFM)	4
3.1.3 Fourier Transform Infrared Spectroscopy (FTIR)	4
3.1.4 UV-Vis Spectroscopy:	5
3.2 Surface Pre-Treatment Processes	5
3.2.1 Ozone Treatment.....	5
3.2.2 Contact Angle Measurement	6
3.3 Lamination.....	7
3.3.1 Sheet lamination Methods	7
3.4 Methodology	11
3.4.1 Preparation of materials.....	11
3.4.2 Lamination process	11
3.4.3 Dog Bone Specimen Preparation	12
3.4.4 Specimen Conditioning.....	15
CHAPTER 4	17
RESULTS	17
4.1 Morphological studies.....	17
4.1.1 Scanning Electron Microscopy (SEM).....	17
4.2 Morphological and Topographical studies.....	18
4.2.1 Atomic Force Microscopy (AFM)	18

4.3	Surface Chemistry.....	19
4.3.1	Fourier Transform Infrared Spectroscopy (FTIR)	19
4.3.2	Wetting studies.....	22
4.3.3	Analysis	28
4.3.4	Surface Energies	29
4.3.5	UV-Vis Spectroscopy	30
4.3.6	PMMA Tensile test.....	35
4.3.7	Non-Laminated Sample	35
4.3.8	Summary of Key Observations.....	42
4.3.9	Non-Laminated Sample	42
	CONCLUSION	44
	REFERENCES	45

LIST OF TABLES

TABLE 1 MATERIALS SELECTION	2
TABLE 2 USAGE	3
TABLE 3 SAMPLE DESIGNATION.....	6
TABLE 4 DIMENSIONS FOR TYPE V SAMPLE	15
TABLE 5 CALCULATION OF SURFACE FREE ENERGIES.....	29
TABLE 6 PROPERTIES DEFINITION.....	35
TABLE 7 COMPARISON OF TENSILE STRENGTH AND STRESS-STRAIN BEHAVIOR OF PMMA SAMPLES	41

TABLE OF FIGURES

FIGURE 1 UV-VIS SPECTROPHOTOMETER.....	5
FIGURE 2 OZONE TREATMENT SETUP	6
FIGURE 3 GONIOMETER FOR MEASURING CONTACT ANGLE	7
FIGURE 4 LAMINATION STACKING.....	7
FIGURE 5 VACUUM BAGGING SETUP.....	9
FIGURE 6 TYPICAL VACUUM BAGGING SETUP.....	10
FIGURE 7 COMPOSITE PRESS.....	11
FIGURE 8 DOG BONE SAMPLE ON AUTOCAD	13
FIGURE 9 LASER CUTTING.....	14
FIGURE 10 UNIVERSAL TENSILE TEST	15
FIGURE 11 DOGBONE SAMPLE DIMENSIONS	15
FIGURE 12 MICROGRAPH OF POLYMETHYL METHACRYLATE (PMMA)	17
FIGURE 13 MICROGRAPH OF POLYURETHANE (PU).....	17
FIGURE 14 AFM RESULTS.....	18
FIGURE 15 BAR CHART OF OZONE TREATED SAMPLES, PORTRAYING VALUES OF ROUGHNESS	19
FIGURE 16 CHEMICAL STRUCTURE OF PMMA.....	19
FIGURE 17 FTIR RESULTS OF PMMA	20
FIGURE 18 CHEMICAL STRUCTURE OF POLYURETHANE (PU).....	20
FIGURE 19 FTIR RESULTS OF PU.....	21
FIGURE 20 FTIR RESULTS OF OZONE TREATED SAMPLES OF PMMA	21
FIGURE 21 VALUE OF CONTACT ANGLE OF UNTREATED POLYMETHYL METHACRYLATE (PMMA), HAVING AN AVERAGE VALUE OF 71.2°	22
FIGURE 22 FIRST VALUE OF CONTACT ANGLE OF TREATED POLYMETHYL METHACRYLATE (PMMA) FOR 15 MINUTES, HAVING AN AVERAGE VALUE OF 51.3°.....	22
FIGURE 23 VALUE OF CONTACT ANGLE OF TREATED POLYMETHYL METHACRYLATE (PMMA) FOR 30 MINUTES.....	22
FIGURE 24 VALUE OF CONTACT ANGLE OF TREATED POLYMETHYL METHACRYLATE (PMMA) FOR 45 MINUTES, HAVING AN AVERAGE OF 46.6°	23

FIGURE 25 VALUES OF CONTACT ANGLE OF TREATED PMMA WITH AND WITHOUT OZONE TREATMENT, WHILE USING WATER AS THE WETTING SOLVENT	23
FIGURE 27 VALUE OF CONTACT ANGLE OF UNTREATED POLYMETHYL METHACRYLATE (PMMA) WITH WATER, HAVING AN AVERAGE VALUE OF 63.75°	24
FIGURE 26 VALUE OF CONTACT ANGLE OF UNTREATED POLYMETHYL METHACRYLATE (PMMA) WITH ETHYLENE GLYCOL, HAVING AN AVERAGE VALUE OF 46.6°	24
FIGURE 28 VALUE OF CONTACT ANGLE OF TREATED POLYMETHYL METHACRYLATE (PMMA) FOR 15 MINUTES WITH WATER, HAVING AN AVERAGE VALUE OF 36.9°	24
FIGURE 29 VALUE OF CONTACT ANGLE OF TREATED POLYMETHYL METHACRYLATE (PMMA) FOR 15 MINUTES WITH ETHYLENE GLYCOL, HAVING AN AVERAGE VALUE OF 14.4°	25
FIGURE 30 VALUE OF CONTACT ANGLE OF TREATED POLYMETHYL METHACRYLATE (PMMA) FOR 30 MINUTES WITH WATER, HAVING AN AVERAGE VALUE OF 29.9°	25
FIGURE 31 VALUE OF CONTACT ANGLE OF TREATED POLYMETHYL METHACRYLATE (PMMA) FOR 60 MINUTES WITH ETHYLENE GLYCOL, HAVING AN AVERAGE VALUE OF 15.3°	25
FIGURE 32 VALUE OF CONTACT ANGLE OF TREATED POLYMETHYL METHACRYLATE (PMMA) FOR 30 MINUTES WITH WATER, HAVING AN AVERAGE VALUE OF 31.6°	26
FIGURE 33 VALUE OF CONTACT ANGLE OF TREATED POLYMETHYL METHACRYLATE (PMMA) FOR 30 MINUTES WITH ETHYLENE GLYCOL, HAVING AN AVERAGE VALUE OF 12.4°	26
FIGURE 34 VALUE OF CONTACT ANGLE OF TREATED POLYMETHYL METHACRYLATE (PMMA) FOR 60 MINUTES WITH ETHYLENE GLYCOL, HAVING AN AVERAGE VALUE OF 28.3°	26
FIGURE 35 VALUE OF CONTACT ANGLE OF TREATED POLYMETHYL METHACRYLATE (PMMA) FOR 60 MINUTES WITH WATER, HAVING AN AVERAGE VALUE OF 36.85°	26
FIGURE 36 VALUE OF CONTACT ANGLE OF TREATED POLYMETHYL METHACRYLATE (PMMA) FOR 75 MINUTES WITH WATER, HAVING AN AVERAGE VALUE OF 32.55°	27
FIGURE 37 VALUE OF CONTACT ANGLE OF TREATED POLYMETHYL METHACRYLATE (PMMA) FOR 75 MINUTES WITH ETHYLENE GLYCOL, HAVING AN AVERAGE VALUE OF 30.5°	27

FIGURE 38 VALUE OF CONTACT ANGLE OF TREATED POLYMETHYL METHACRYLATE (PMMA) FOR 90 MINUTES WITH WATER, HAVING AN AVERAGE VALUE OF 37.55°	27
FIGURE 39 VALUE OF CONTACT ANGLE OF TREATED POLYMETHYL METHACRYLATE (PMMA) FOR 90 MINUTES WITH ETHYLENE GLYCOL, HAVING AN AVERAGE VALUE OF 26.35°.....	28
FIGURE 40 COMPARISON GRAPH OF VALUE OF CONTACT ANGLE ACHIEVED BY USING WATER AND ETHYLENE GLYCOL AS WETTING SOLVENTS	28
FIGURE 41 VALUES AND EQUATIONS FOR CALCULATION OF SURFACE ENERGIES.....	29
FIGURE 42 SURFACE FREE ENERGY VS TIME GRAPH FOR UNTREATED AND OZONE TREATED SAMPLES AT 15, 30 AND 45 MINUTES.....	30
FIGURE 43 COMPARISON GRAPH OF UV-VIS SPECTROSCOPY RESULTS WITH SURFACE PRE-TREATMENT OF DIFFERENT INTERVALS	31
FIGURE 44 BAR GRAPH SHOWING MAXIMUM VALUES OF TRANSMITTANCE ACHIEVED	31
FIGURE 45 SAMPLE 1	32
FIGURE 46 SAMPLE 2	33
FIGURE 47 SAMPLE 3	34
FIGURE 48 SAMPLE 4	34
FIGURE 49 STRESS STRAIN GRAPH OF NON-LAMINATED SAMPLE	36
FIGURE 50 STRESS-STRAIN GRAPH OF SAMPLE 1.....	37
FIGURE 51 STRESS-STRAIN GRAPH OF SAMPLE 2.....	38
FIGURE 52 STRESS-STRAIN GRAPH OF SAMPLE 3.....	39
FIGURE 53 STRESS-STRAIN GRAPH OF SAMPLE 4.....	40
FIGURE 54 STRESS STRAIN GRAPH OF SAMPLE 5	41
FIGURE 55 TENSILE TEST GRAPH OVERLAPPING FOR COMPARISON	43

CHAPTER 1

INTRODUCTION

1.1 Background

Poly(methyl methacrylate) (PMMA), commonly known as acrylic or plexiglass, stands out as a highly versatile polymer with a myriad of applications across diverse industries. Its exceptional optical clarity, lightweight nature, UV resistance, and ease of fabrication make it a favored material in the optical industry for lenses and light guides, the automotive sector for durable lighting components, construction and architecture for windows and facades, medical applications for biocompatible devices, and advertising for vibrant signage. PMMA's unique combination of properties contributes to its widespread use, offering solutions in design, durability, and functionality for a range of products.

Ozone Treatment is a surface pre-treatment technique to improve wettability and spreading ability of liquid on a surface. It introduces different functional groups on the surface and oxidizes oxygen into ozone, lowering the value of contact angle.

Lamination is the process of creating a material in several layers with the goal of using different materials—like plastic—to improve the composite material's strength, optical transparency stability, sound insulation, look, and other qualities. A laminate is a material or object that is put together in layers using adhesives, heat, pressure, or welding. There are several machine presses, coating machines, and calendaring apparatuses in use. [4]

Tensile testing plays a pivotal role in understanding and optimizing the mechanical behavior of PMMA. This method provides critical insights into the material's response to applied forces, aiding in the assessment of its strength, elasticity, ductility, and toughness. By conducting tensile tests, researchers and engineers can determine the ultimate tensile strength, elastic modulus, elongation at break, and other crucial mechanical properties. These insights are essential for quality control in manufacturing, ensuring that PMMA products meet specific standards and performance criteria. Moreover, the data obtained from tensile testing guides material selection, enabling the development of PMMA-based

products with enhanced reliability and performance across various industries. In the study of laminated glass, the tensile properties of interlayer materials play a crucial role in determining the overall performance and durability of the composite structure. This research focuses on the tensile testing of laminated samples comprising PMMA (Polymethyl Methacrylate) with polyurethane (PU) used both as a film and in adhesive form. By investigating the tensile strength and stiffness of these laminated samples, we aim to understand the mechanical behavior and durability of the interlayer under varying conditions. The study compares the mechanical properties of unaged specimens with those subjected to environmental factors such as thermal cycles, high temperatures, and moisture. The results reveal how the strain rate and aging processes affect the tensile strength and stiffness of the PMMA-PU interlayer, providing insights into the material's suitability for applications requiring high performance and resilience. Notably, the sample utilizing polyurethane in adhesive form demonstrated superior tensile strength, highlighting its potential advantages in laminated glass applications.

1.2 Objectives

- Implementation of an effective Surface Pre-Treatment to achieve a clean surface, free of contaminants
- Development of a Lamination Process to gain an optical transparency of greater than 90%
- Characterization of laminates through mechanical tests such as Tensile test, Shear test, Impact Test

CHAPTER 2

LITERATURE REVIEW

Baldan's research paper describes the phenomena of adhesion in bonded joints. It gives information about contact angle measurements, which was one of the first steps we performed on PMMA. Through this, we came to know about wettability characteristics. Moreover, ensuring that the surface is clean and free of contaminants is essential to obtain accurate measurements. It highlights effective surface treatments including etching. This improves the reactivity of the surface and wetting behavior as well. [1]

A technical inquiry report issued by the Defense Systems Information Analysis Centre (DSAIC) discusses materials utilized in the transparencies of an aircraft. For canopies, it suggests laminated acrylics and polycarbonates. Canopy's complicated structure and shape can be maintained through processes such as drape molding and vacuum forming. Recommended materials for interlayer are polyurethane and silicon. [2]

TABLE 1: MATERIALS SELECTION

Material Suggested for Canopies	Laminated Acrylics and Polycarbonates
Process for maintaining curved shape of Canopy	Drape Molding Vacuum Forming
Materials Suggested for Interlayer	Polyurethane Silicon

The third source that we have acquired is based on a case description. The materials that are put forward here are polycarbonate and acrylic for bonding in the form of a film and the adhesive used can be polyurethane. It describes a thermoforming process. Furthermore, it is identified that polycarbonate is the most suitable material for the construction of canopies, and to tolerate the high impact resistance. Another thing pointed out is that the elastic nature of the polyurethane layer is deemed to be good for countering the dimensional difference between layers that leads to the production of shear forces. [3]

TABLE 2: USAGE

Use	Material Suggested
Bonding	Polycarbonate Acrylic
Adhesive	Polyurethane

'Characterization and modeling of poly(methyl methacrylate) and thermoplastic polyurethane for the application in laminated setups' by Andreas Rühl a, Stefan Kollinga , and Jens Schneiderthe indicates that the study focuses on transparent polymeric laminates, which are increasingly being utilized as substitutes for traditional glass and laminated safety glass. The objective is to develop reliable and efficient prediction and modeling techniques, particularly for numerical simulations. The specific materials investigated in this work are poly(methyl methacrylate) (PMMA) plies combined with a thermoplastic polyurethane (TPU) interlayer.

The research employs a combination of experimental and numerical methods. Uniaxial tensile tests and dynamic mechanical thermal analysis (DMTA) are conducted to understand the strain-rate and temperature-dependent behavior of the materials. Additionally, adiabatic heating of the TPU interlayer is observed using infrared (IR) surveillance.

2.1 Material

Two polymer-based materials were mainly performed for carrying out this project. These were:

1. Polymethyl methacrylate (PMMA)
2. Polyurethane (PU)

EXPERIMENTAL WORK

3.1 Characterizations

3.1.1 Scanning Electron Microscopy (SEM)

SEM samples are painstakingly prepared by going through several stages. To preserve its integrity, the specimen is first gathered and, if needed, cleaned properly for accurate results. After that, the sample is mounted into a holder, moisture is eliminated by dehydration, and structural damage is avoided by critical point drying. To improve conductivity and image clarity, a conductive coating was added. Lastly, before analysis, the prepared sample is handled carefully to prevent contamination. By following these procedures, the SEM images reveal precise information about the composition and structure of the sample.

3.1.2 Atomic Force Microscopy (AFM)

The samples were cleaned with ethanol and cut into a small standard size in workshop. The cantilever was carefully selected, and probe was installed in the AFM head. Then, the microscope's laser beam was focused onto the backside of the AFM cantilever. We secured our sample onto the AFM stage, and slowly lowered the probe towards the sample surface using AFM's controls. After setting the scan parameters, AFM software acquired data such as surface topography.

3.1.3 Fourier Transform Infrared Spectroscopy (FTIR)

For the sample preparation little pieces of PMMA and polyurethane were cut. Then those pieces are placed in the KBr powder and then pressed into pellets by using a manual hydraulic press. The pallets are placed in the sample holder of FTIR setup and the results are obtained.

3.1.4 UV-Vis Spectroscopy:

The main objective of our research project is to achieve an optical transparency of 90%. This was shown by carrying out UV-Vis spectroscopy. It was achieved by observing values of transmittance, which was gained by passing UV-light through the sample. Initially, a base sample of PMMA was used and its readings were taken. It helped to account for any errors made later. The sample was placed in the cuvette holder and then inserted into the spectrophotometer. Values were portrayed at multiple wavelengths.



FIGURE 1 UV-VIS SPECTROPHOTOMETER

3.2 Surface Pre-Treatment Processes

3.2.1 Ozone Treatment

Surface Pre-Treatment was carried out at 32W power using Ultraviolet (UVC) lamp. This treatment is carried out to obtain a clean surface, free of contaminants. The samples were initially prepared by cleaning them. It was attained by soaking a tissue paper with ethanol and applying it on the surface of PMMA. It introduces functional groups on the surface and causes oxidation of oxygen into ozone.

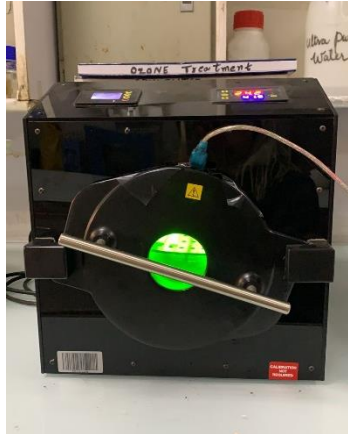


FIGURE 2 OZONE TREATMENT SETUP

To study the effect of time on wetting characteristics ozone treatment was carried out at different time intervals, presented in Table 3.

TABLE 3 SAMPLE DESIGNATION

Sample Number	Time
1	15 Minutes
2	30 Minutes
3	45 Minutes
4	60 Minutes
5	75 Minutes
6	90 Minutes

3.2.2 Contact Angle Measurement

It was measured by using an instrument, named goniometer. The values were obtained using software called Kruss Advance. This goniometer has been manufactured in Germany, and the version is DSA25. Before measurement, it was ensured that the surface of the solid is dry, clean and free of contaminants. Sample was fixed on the horizontal stage of the optical tensiometer. Blue light was focused more on it as it undergoes lesser scattering phenomena on edges as compared to white light. It was also checked that the goniometer is calibrated using a standard reference material, with a known value of contact angle. A tiny droplet of water was placed on the surface of the sample through the syringe. Images were captured by clicking the HD camera. The software, Kruss Advance took the reading after the image was inserted, when it was set to sessile mode. In a situation where the value of contact angle was

high, the mode of the software was changed to ellipse model. Measurements were taken at different points to increase their accuracy, and their average value was calculated.

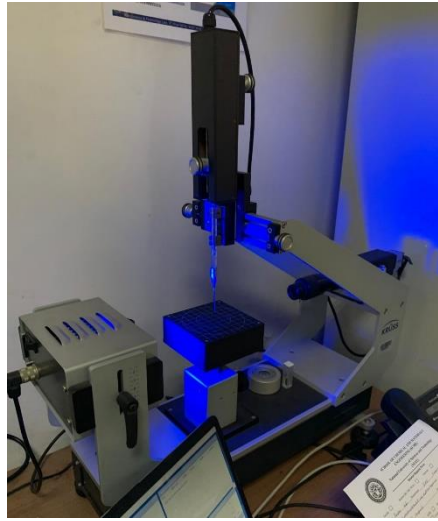


FIGURE 3 GONIOMETER FOR MEASURING CONTACT ANGLE

3.3 Lamination

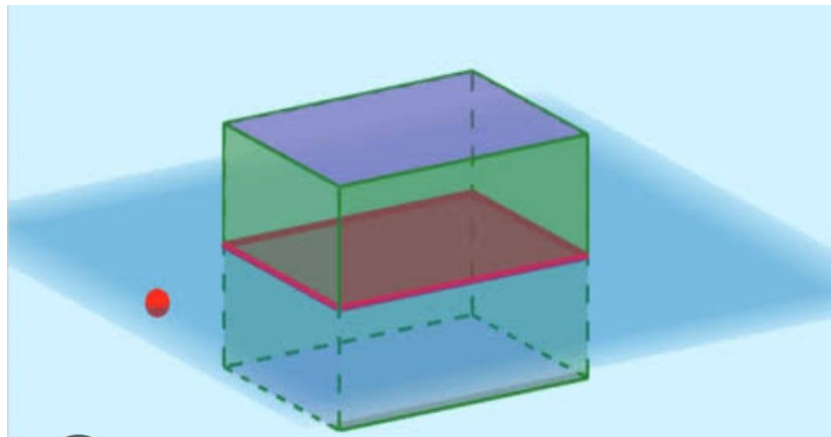


FIGURE 4 LAMINATION STACKING

3.3.1 Sheet lamination Methods

3.3.1.1 Thermal joining

The materials are laminated together under heat and pressure. Once the materials—which are often chemically similar—are heated over their glass transition temperature (T_g), chains of partially melted polymers diffuse into one another under the applied stress, forming a bond. The partially mixed polymers of both substrates make up the interphase that is thus generated. Occasionally, plasticizing solvents are used to reduce the T_g . The polymeric

materials, different in nature, are usually non-miscible and hence it is difficult or impossible to laminate them by thermal joining method. Also, polymers have lower entropy of mixing and cannot accommodate enthalpy changes. Therefore, this method of lamination which relies on partial mixing of polymers is not suitable for chemically different polymers. However, for partially miscible polymers this method results in gradual change in diffraction index.

3.3.1.2 Lamination By Adhesive bonding

PMMA sheets were bonded by using polyurethane adhesive. Adhesive forms electrostatic interactions with the pre-treated adjacent layers and form a strong interface.

At first, the liquid adhesive was cast onto the PMMA sheets. They were allowed to cure for 24 hours having a 40kg load placed on them to aid the bonding process.

To incorporate thickness control of the laminate and to improve the overall curing of the PU adhesive vacuum bagging was used.

3.3.1.3 Vacuum bagging

One popular and useful method for applying pressure to composite materials is using hoover bags. In comparison to weights or clamps, the pressure is extremely high and constant. The earth's atmosphere presses down on everything at a rate of about 14 pounds per square inch, which explains why it works. Naturally, we are accustomed to it so we don't feel it that much normally.

Vacuum bagging has enormous power, but it also presents several difficulties. The bag needs to be reasonably leak-proof, and the plastic shouldn't press unevenly against the workpiece since this could cause major harm. Because plastic film is not so robust, it's simple for the bag to burst on its own. Numerous other options are possible. Many excellent items and methods have been developed during decades of development to make the process simple and efficient [5].

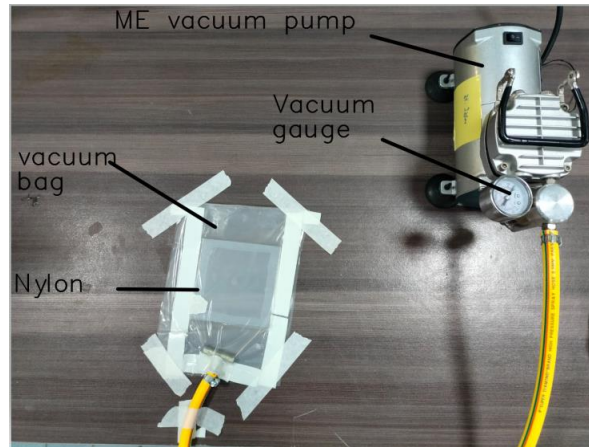


FIGURE 5 VACUUM BAGGING SETUP

3.3.1.4 Bag Film

There is a vast array of materials, thicknesses, widths, and stretch abilities available for bag film. Make sure it is rated for the temperature if you plan to cure it at a high level. Unless you have a very strong reason to do differently, we would start with a conventional nylon/blend bagging film. Vacuum bagging is said to be made simpler by several very high elongation bag films (Stretch Lon from Airtech is one example). This content can be helpful in some circumstances, but it also raises several other possible issues and seems to overlook several technical mistakes that would be better off knowing how to address correctly. Its ability to stretch makes it simple to conform to an intricate part, but the act of stretching itself has the potential to cause material to slide under the bag and reduce the amount of pressure the bag can apply to the part. Avoid using the elastic bag for infusion as it may cause many problems. Start small and thoroughly understand the pleating elements before experimenting with the more intricate details. [5]

3.3.1.5 Breather/ Bleeder

A sort of 'breather' fabric, underneath your bag to spread the vacuum. Usually, this is a fuzzy, fluffy, non-woven sheet. It is available in many thicknesses. Stick with the thin material (4 oz, 150g, or so), as it's easier to work with and won't absorb a lot of resin. This breather, also known as a "bleeder," is necessary to prevent excess resin from adhering to your part. It serves two purposes. Usually, this is a perforated release film or a coated peel ply (often green or blue) with a release agent applied that makes it easy to peel off your part. [5]

3.3.1.6 Peel ply.

Primarily composed of nylon, peel ply can also contain polyester and other coated materials. It presses up against the component to leave a smooth surface ready for finishing or secondary bonding. Coated peel piles are excellent and have an easy release. A coated peel ply can be utilized to aid in the removal of resin-covered surface-flow media during infusion. If you are utilizing an uncoated nylon peel ply for wet-layup or pre-preg, it is best—no, necessary—to use release films. This will reduce the quantity of resin that the breather/bleeder is able to absorb and allow the breather fabric to separate, revealing the portion that is covered in peel-ply. [5]

3.3.1.7 Sealant tape:

The bag will be adhered to the mold or the area where vacuum-bagged laminate is being applied using sealant tape. It resembles sticky tape like Silly Putty and is packaged in rolls with paper backing in between layers. When purchasing a case or several rolls of sealant tape, take extra care to keep it chilled and to maintain the rolls' orderly stacking and alignment with the cardboard tubes.

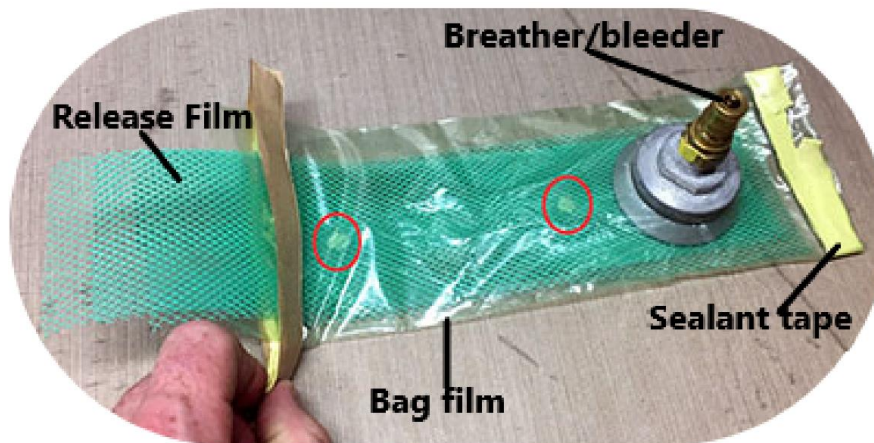


FIGURE 6 TYPICAL VACUUM BAGGING SETUP

3.3.1.8 Lamination By Hot press:

A specialized tool used in the creation of composite materials is a composite press, often known as a hot press. It works by bonding various layers of materials, such as polymers, metals, or fibers, together at the same time with pressure and heat to create a cohesive

structure with improved qualities. To establish strong, consistent bonding, the press usually has heated plates that provide uniform temperature distribution and accurate pressure control. Composite presses are frequently used in sectors where producing high-performance, lightweight, and durable materials is essential, such as aerospace, automotive, and construction. Temperature, pressure, and pressing time are just a few of the process variables that are carefully adjusted to customize the properties of the composite to meet application-specific needs. [6]

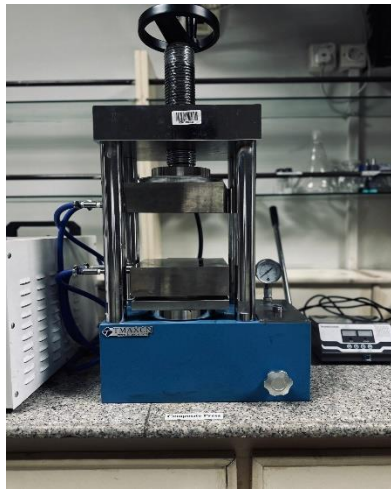


FIGURE 7 COMPOSITE PRESS

3.4 Methodology

3.4.1 Preparation of materials

Wipe the PMMA and PU sheets with a mixture of ethanol and Lukewarm water to clear any glue residue and contaminants from the surface of the PMMA tiles. Let the samples dry for some time and then proceed with the lamination process.

Additionally, the surface is also pretreated to increase its surface energy. This will lead to better adhesion of the laminated surfaces.

3.4.2 Lamination process

- The first step of the lamination process is stacking. Carefully place the PU film between two PMMA sheets, ensuring proper alignment.
- Ensure that the sheets are perfectly aligned to avoid misalignment during the pressing process.

- Use alignment tools if necessary.
- Close the hot press and apply the pre-set temperature and pressure.
- Maintain these conditions for the required duration. Typical pressing time ranges from 3-4 hr.
- Monitor the process to ensure consistent application of heat and pressure.

After letting the laminates cool properly remove them from the hot press. After this a visual inspection is done to check whether the PMMA sheets have adhered or not. This followed by checking the defects under a microscope. [7]

3.4.3 Dog Bone Specimen Preparation

Adherence to ASTM D638-22 specifications for Type V specimen dogbone samples was achieved by using a laser cutting machine for precision and consistency. ASTM D638-22 specifies the standard test method for tensile properties of plastics, providing guidelines for the preparation, conditioning, and testing of plastic materials to ensure uniformity and reproducibility of results. The Type V specimen is one of the various specimen geometries defined in the standard, tailored for testing thin plastic films or sheets with thicknesses up to 4 mm. The dimensions and tolerances for Type V specimens are meticulously detailed in the standard to ensure accurate and reliable tensile testing. Utilizing a laser cutting machine ensures that the samples conform to these stringent specifications, thereby enhancing the reliability of the tensile property data obtained.

The design for the Type V specimen was created using AutoCAD to ensure precise adherence to ASTM D638-22 dimensions. The drawing process began by setting up the AutoCAD workspace with appropriate units and scales. The central section of the dogbone sample, which is the narrowest part, was drawn first, ensuring it had a consistent width as specified by the standard. The ends of the specimen were then sketched, gradually widening from the central section to the gripping areas to ensure uniform stress distribution during tensile testing. These end sections were drawn as symmetrical arcs to create the smooth transition required by the standard.

Specific dimensions, such as the overall length, width of the narrow section, and radius of the arcs, were input precisely according to ASTM D638-22 guidelines. Each line and curve was

verified for accuracy, ensuring that the critical dimensions and tolerances were met. The final AutoCAD design included annotations and dimensions for reference, facilitating easy verification before the laser cutting process.

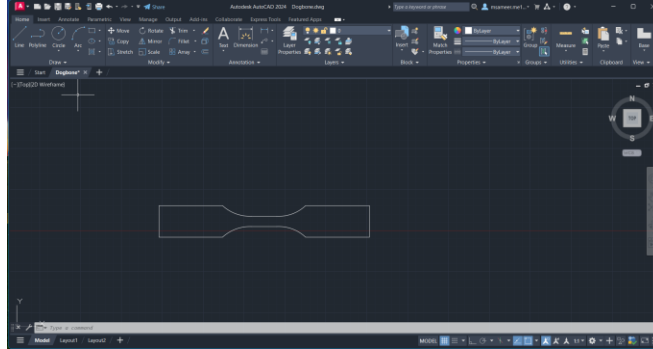


FIGURE 8 DOG BONE SAMPLE ON AUTOCAD

Once the design was completed, it was saved in a format compatible with the laser cutting machine software. The laser cutting machine then used this design to cut the plastic sheets into Type V dogbone specimens with high precision, ensuring that all samples were consistent and met the stringent requirements of the ASTM D638-22 standard. This methodical approach in designing and cutting the specimens ensured their suitability for accurate tensile property testing

The process of cutting PMMA on the SKL 6090 laser cutter machine began by transferring the AutoCAD design file to the machine's control software. The PMMA sheet was securely placed on the cutting bed of the SKL 6090, ensuring it was flat and stable to achieve precise cuts. The machine settings were configured based on the material properties of PMMA and the thickness of the sheet being used. The laser power was set to 60 watts, which is suitable for cutting PMMA with a thickness of up to 4 mm, providing clean and accurate edges without causing significant melting or deformation.



FIGURE 9 LASER CUTTING

After setting the power, the cutting speed and frequency were adjusted to optimize the cutting quality. The appropriate speed was determined to balance between cutting efficiency and the quality of the edges, typically set to a moderate pace to prevent charring or excessive heat buildup. Once all parameters were set, a test cut was performed on a small section of the PMMA sheet to ensure the settings were correct and to make any necessary adjustments.

With the parameters verified, the full cutting process was initiated. The laser cutter followed the AutoCAD design precisely, using the high-intensity laser beam to vaporize the PMMA along the designated paths. The extraction system was activated to remove fumes and debris generated during cutting, ensuring a clean working environment and preventing any contamination of the cut edges. The process was monitored closely to ensure consistent quality and to address any issues that might arise. Once the cutting was complete, the finished Type V specimens were carefully removed from the cutting bed, inspected for dimensional accuracy, and cleaned of any residual material. This meticulous process ensured that the PMMA dogbone samples met the stringent requirements of ASTM D638-22, ready for subsequent tensile testing.

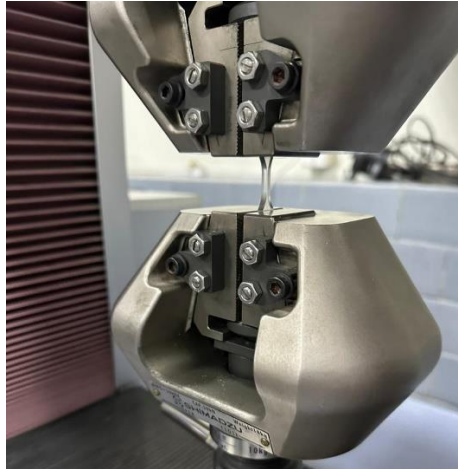
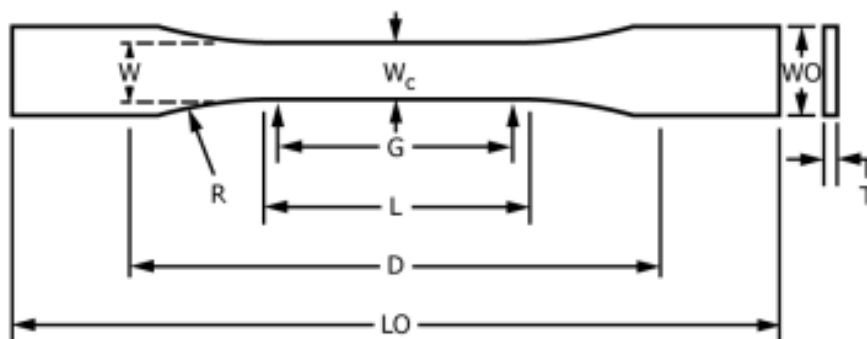


FIGURE 10 UNIVERSAL TENSILE TEST

3.4.4 Specimen Conditioning



TYPES I, II, III & V

FIGURE 11 DOGBONE SAMPLE DIMENSIONS

TABLE 4 DIMENSIONS FOR TYPE V SAMPLE

Dimensions (see drawings)	Type V	Tolerances
W—Width of narrow section	3.18 (0.125)	±0.5 (±0.02)
L—Length of narrow section	9.53 (0.375)	±0.5 (±0.02)
WO—Width overall, minG	9.53 (0.375)	+ 3.18 (+ 0.125)
LO—Length overall, min	63.5 (2.5)	no max (no max)
G—Gage length	7.62 (0.300)	±0.25 (±0.010)

D—Distance between grips	25.4 (1.0)	$\pm 5 (\pm 0.2)$
R—Radius of fille	12.7 (0.5)	$\pm 1 (\pm 0.04)$

RESULTS

4.1 Morphological studies

4.1.1 Scanning Electron Microscopy (SEM)

The micrographs depicted that the surface of Polymethyl methacrylate (PMMA) and polyurethane (PU) were smooth. Rough textures or defects of any sort were not observed on it. It also gave us an indication that our samples are suitable for performing the process of lamination and achieving a maximum value of transparency.

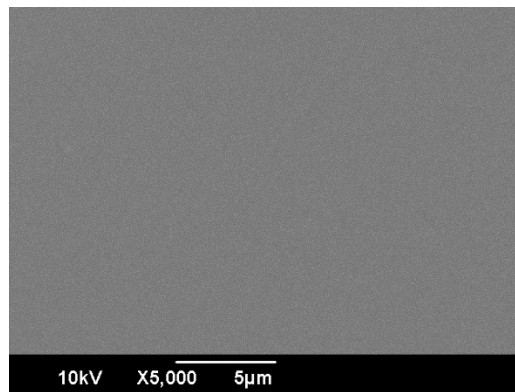


FIGURE 12 MICROGRAPH OF POLYMETHYL METHACRYLATE (PMMA)

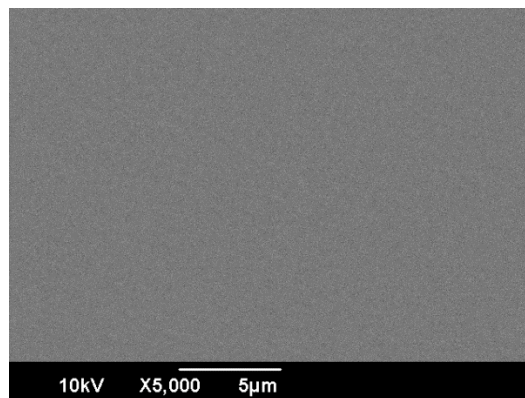


FIGURE 13 MICROGRAPH OF POLYURETHANE (PU)

4.2 Morphological and Topographical studies

4.2.1 Atomic Force Microscopy (AFM)

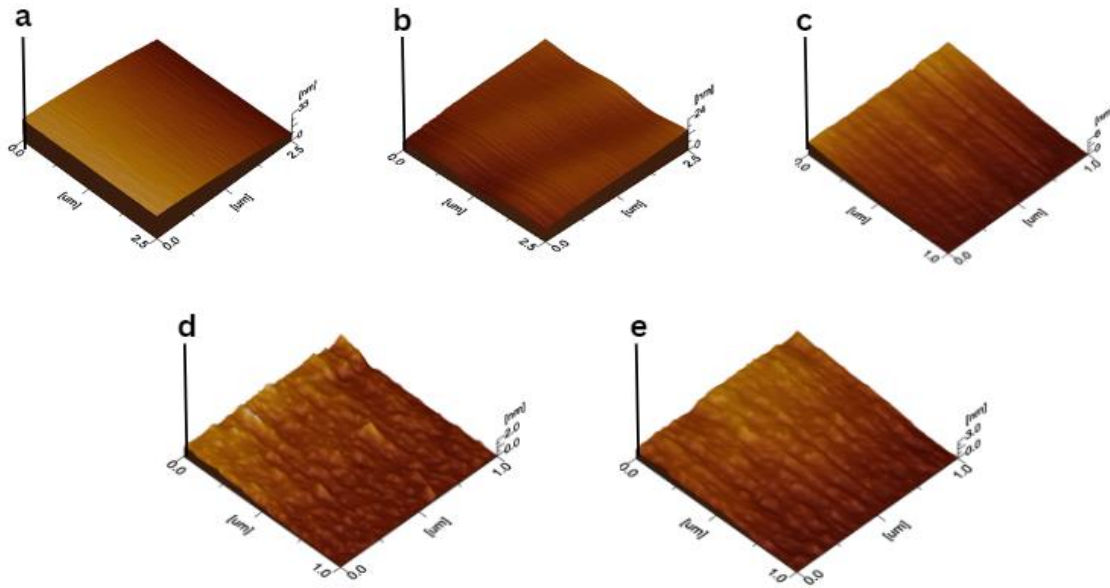


FIGURE 14 AFM RESULTS

- a) PU MEMBRANE b) PMMA SHEET c) 15 MINUTES OZONE TREATED PMMA
d) 30 MINUTES OZONE TREATED PMMA e) 45 MINUTES OZONE TREATED PMMA

Surface topographies of different ozone treated samples was observed. It was found out that at 30 minutes, differences in values of dimensions became the lowest, increasing uniformity. This is effective for a surface with better wettability and adhesion.

The graph below depicts that at 30 minutes of ozone treatment, values of Ra (arithmetic average roughness), Rq (root mean square roughness) and Rz (average maximum height of the profile) were found to be the lowest.

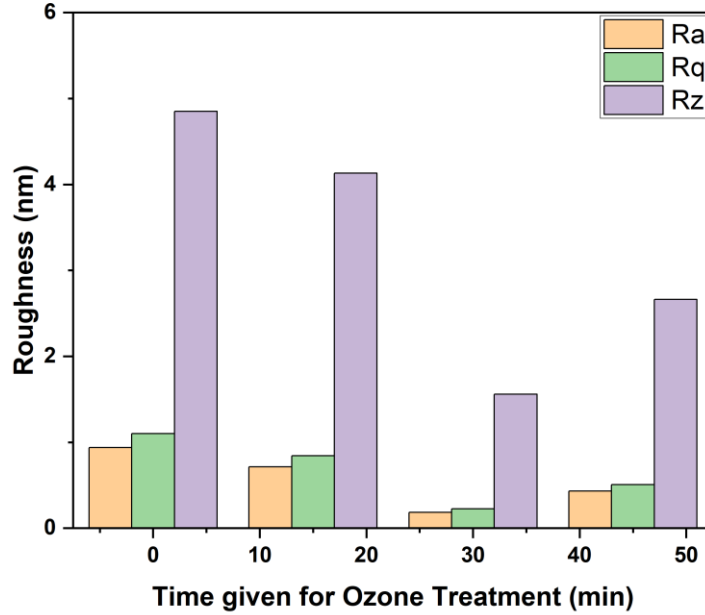


FIGURE 15 BAR CHART OF OZONE TREATED SAMPLES, PORTRAYING VALUES OF ROUGHNESS

4.3 Surface Chemistry

4.3.1 Fourier Transform Infrared Spectroscopy (FTIR)

Chemical bonds present in PMMA. All the bonds shown in it were also present in the FTIR results obtained that are C=O, C-O, C-C.

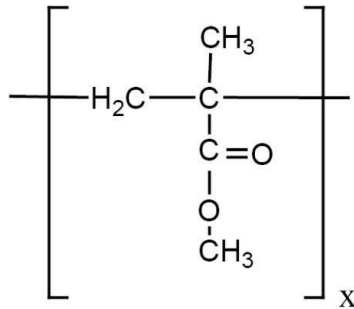


FIGURE 16 CHEMICAL STRUCTURE OF PMMA

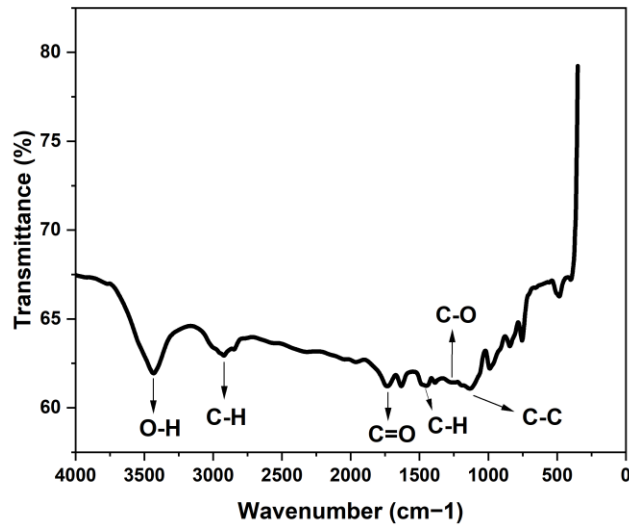


FIGURE 17 FTIR RESULTS OF PMMA

Figure 20 portrays the chemical bonds in Polyurethane (PU). Against different wavenumbers and peaks, chemical bonds that were present are C=O, N-H, C-O, C-H, C-N.

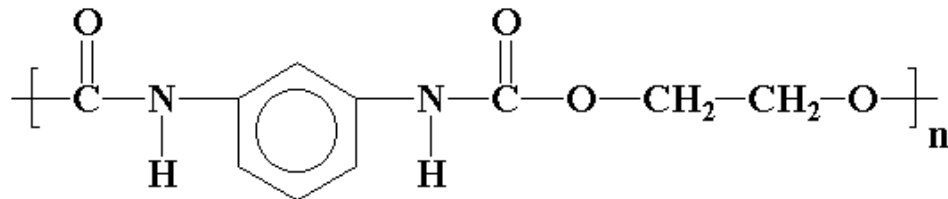


FIGURE 18 CHEMICAL STRUCTURE OF POLYURETHANE (PU)

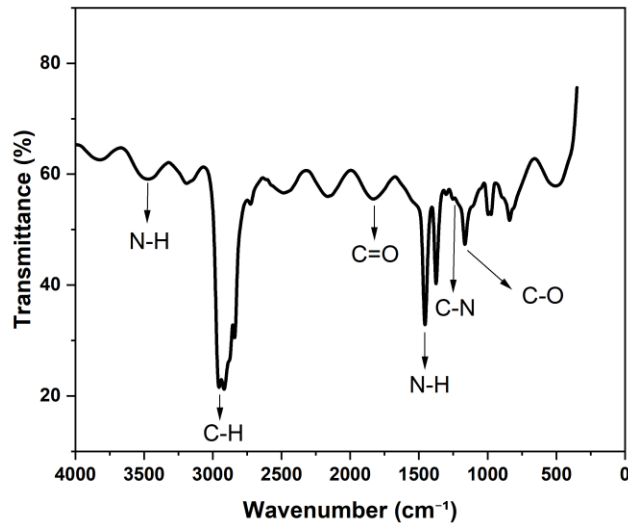


FIGURE 19 FTIR RESULTS OF PU

To analyze the surface chemistry of ozone treated samples, their FTIR was carried out. When ozone was treated for 15 minutes, the functional group of C=O was missing, at 30 minutes surface pre-treatment, absence of C=C group was observed and the functional group of C-H was missing, when ozone treated for 45 minutes.

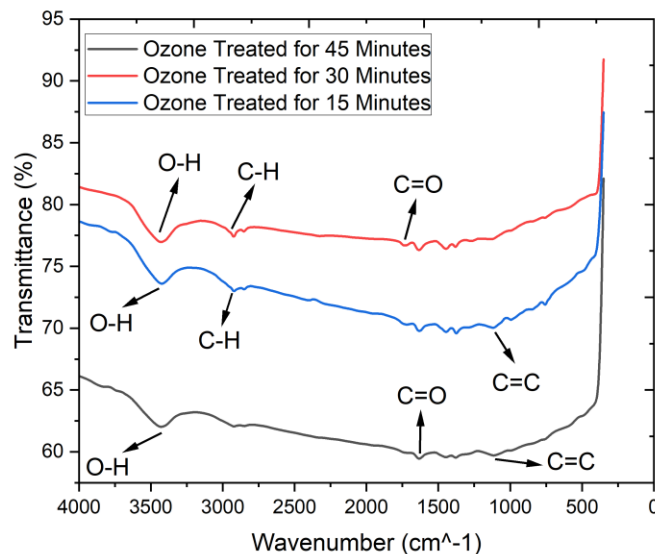


FIGURE 20 FTIR RESULTS OF OZONE TREATED SAMPLES OF PMMA

4.3.2 Wetting studies

4.3.2.1 Contact Angle Measurements



FIGURE 21 VALUE OF CONTACT ANGLE OF UNTREATED POLYMETHYL METHACRYLATE (PMMA), HAVING AN AVERAGE VALUE OF 71.2°

After carrying out ozone treatment at different time intervals, contact angle was measured by placing a drop of water.

The results obtained have been presented below:

After Performing Ozone Treatment for 15 Minutes:



FIGURE 22 FIRST VALUE OF CONTACT ANGLE OF TREATED POLYMETHYL METHACRYLATE (PMMA) FOR 15 MINUTES, HAVING AN AVERAGE VALUE OF 51.3°

After Performing Ozone Treatment for 30 Minutes:

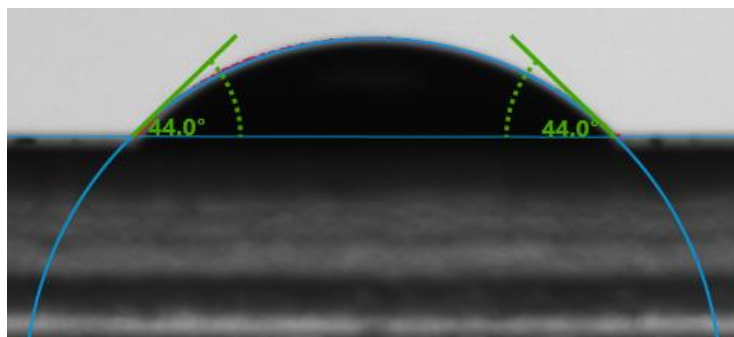


FIGURE 23 VALUE OF CONTACT ANGLE OF TREATED POLYMETHYL METHACRYLATE (PMMA) FOR 30 MINUTES

After Performing Ozone Treatment for 45 Minutes:



FIGURE 24 VALUE OF CONTACT ANGLE OF TREATED POLYMETHYL METHACRYLATE (PMMA) FOR 45 MINUTES, HAVING AN AVERAGE OF 46.6

It can be observed that the value of contact angle is the highest, without performing ozone treatment. This indicated that the surface has contaminants on it. As the amount of time provided for surface pretreatment increases, value of contact angle decreases, enhancing the phenomena of wettability. However, when ozone treatment was performed for 45 minutes, contact angle started to increase again in number. The reasons associated with this can be from the changes taking place during UV light absorption, including the formation of carboxylic acid end-groups, terminal vinyl groups, phenols and the evolution of CO and CO₂. [5]

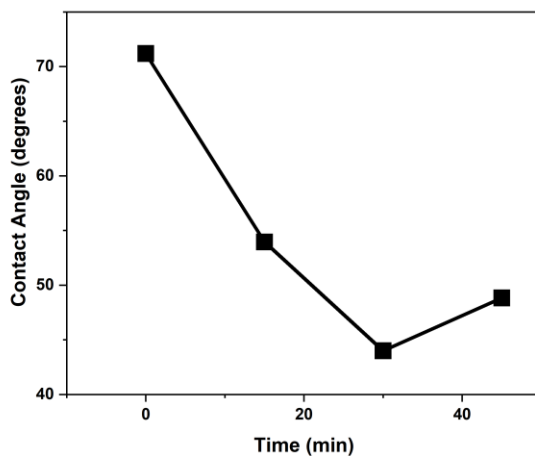


FIGURE 25 VALUES OF CONTACT ANGLE OF TREATED PMMA WITH AND WITHOUT OZONE TREATMENT, WHILE USING WATER AS THE WETTING SOLVENT

The next step taken was to measure values of contact angle by placing a drop of ethylene glycol, instead of water at different time intervals. Values were also calculated with water to draw effective comparisons. The results have been pasted below:

As received:

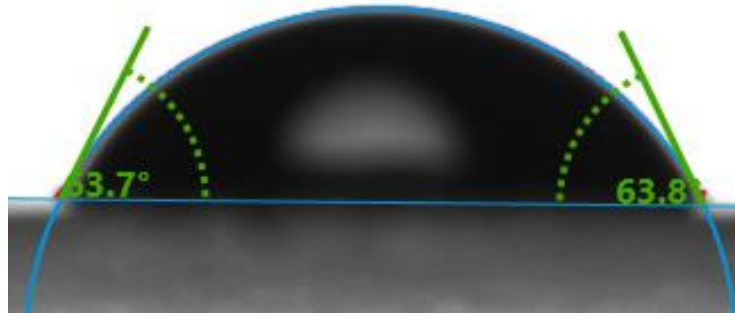


FIGURE 27 VALUE OF CONTACT ANGLE OF UNTREATED POLYMETHYL METHACRYLATE (PMMA) WITH WATER, HAVING AN AVERAGE VALUE OF 63.75°

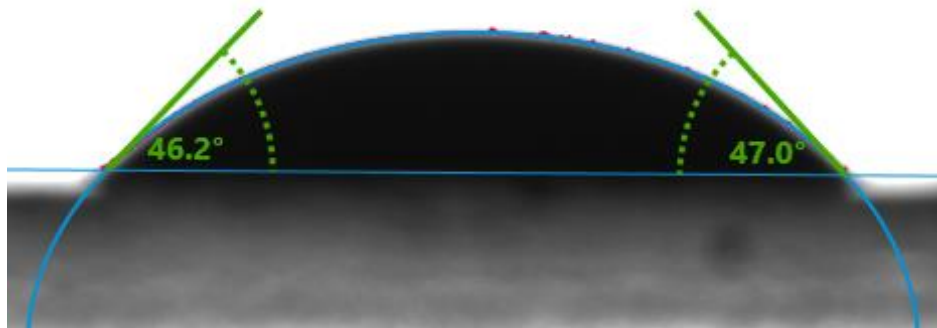


FIGURE 26 VALUE OF CONTACT ANGLE OF UNTREATED POLYMETHYL METHACRYLATE (PMMA) WITH ETHYLENE GLYCOL, HAVING AN AVERAGE VALUE OF 46.6°

After performing Ozone Treatment for 15 Minutes:

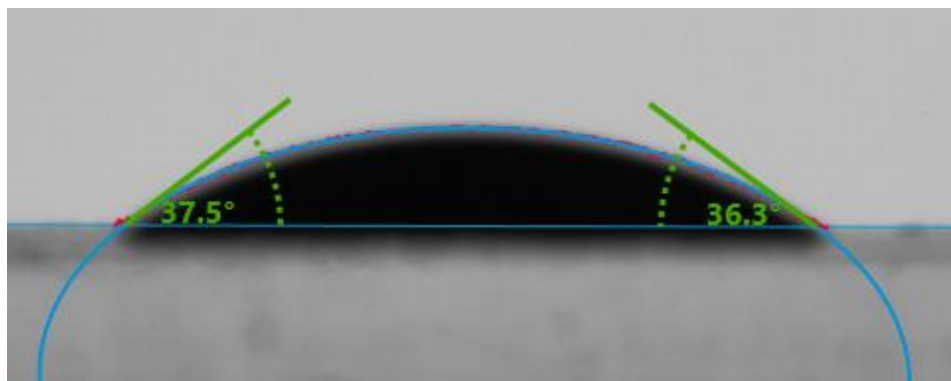


FIGURE 28 VALUE OF CONTACT ANGLE OF TREATED POLYMETHYL METHACRYLATE (PMMA) FOR 15 MINUTES WITH WATER, HAVING AN AVERAGE VALUE OF 36.9°

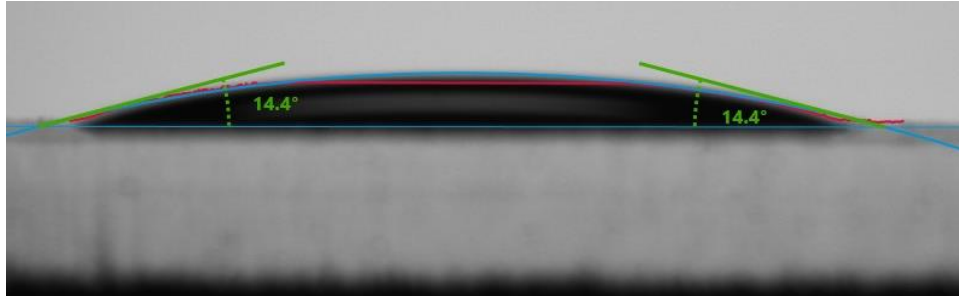


FIGURE 29 VALUE OF CONTACT ANGLE OF TREATED POLYMETHYL METHACRYLATE (PMMA) FOR 15 MINUTES WITH ETHYLENE GLYCOL, HAVING AN AVERAGE VALUE OF 14.4°

After performing Ozone Treatment for 30 Minutes:

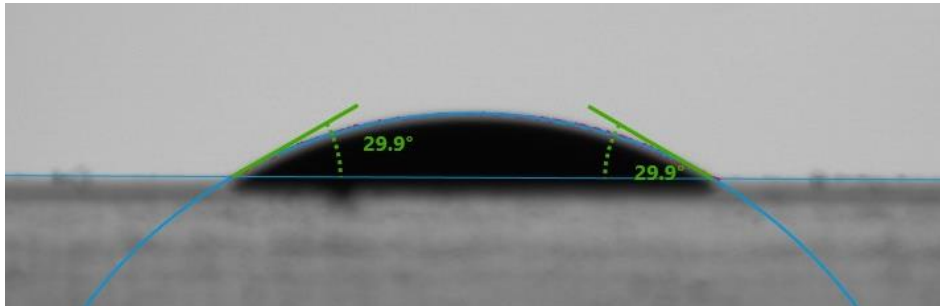


FIGURE 30 VALUE OF CONTACT ANGLE OF TREATED POLYMETHYL METHACRYLATE (PMMA) FOR 30 MINUTES WITH WATER, HAVING AN AVERAGE VALUE OF 29.9°

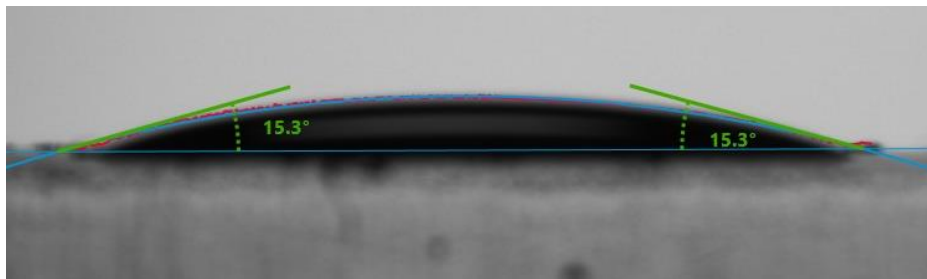


FIGURE 31 VALUE OF CONTACT ANGLE OF TREATED POLYMETHYL METHACRYLATE (PMMA) FOR 60 MINUTES WITH ETHYLENE GLYCOL, HAVING AN AVERAGE VALUE OF 15.3°

After performing Ozone Treatment for 45 Minutes:

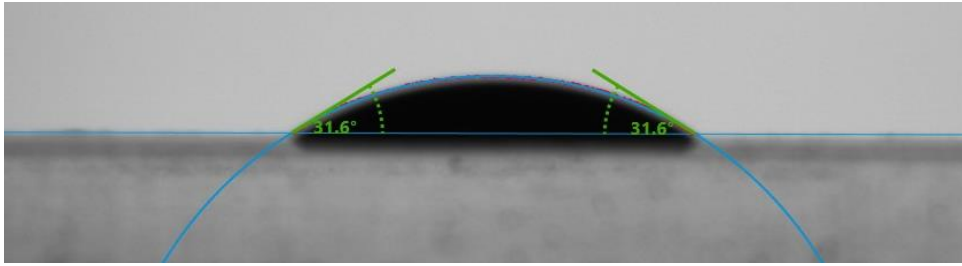


FIGURE 32 VALUE OF CONTACT ANGLE OF TREATED POLYMETHYL METHACRYLATE (PMMA) FOR 30 MINUTES WITH WATER, HAVING AN AVERAGE VALUE OF 31.6°

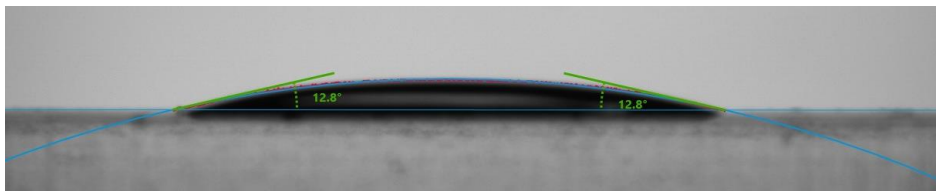


FIGURE 33 VALUE OF CONTACT ANGLE OF TREATED POLYMETHYL METHACRYLATE (PMMA) FOR 30 MINUTES WITH ETHYLENE GLYCOL, HAVING AN AVERAGE VALUE OF 12.4°

After performing Ozone Treatment for 60 Minutes:



FIGURE 35 VALUE OF CONTACT ANGLE OF TREATED POLYMETHYL METHACRYLATE (PMMA) FOR 60 MINUTES WITH WATER, HAVING AN AVERAGE VALUE OF 36.85°

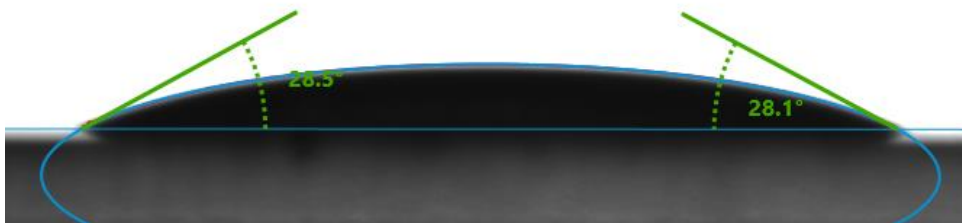


FIGURE 34 VALUE OF CONTACT ANGLE OF TREATED POLYMETHYL METHACRYLATE (PMMA) FOR 60 MINUTES WITH ETHYLENE GLYCOL, HAVING AN AVERAGE VALUE OF 28.3°

After performing Ozone Treatment for 75 Minutes:

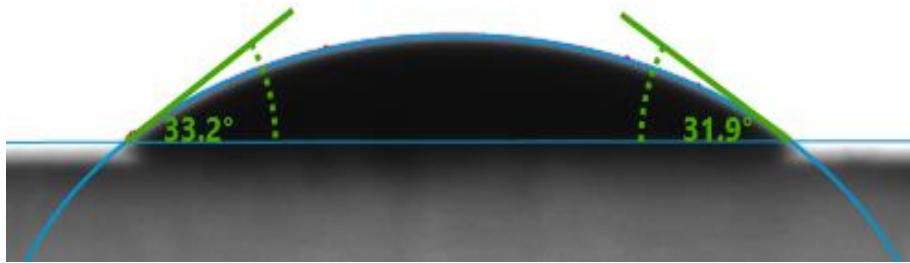


FIGURE 36 VALUE OF CONTACT ANGLE OF TREATED POLYMETHYL METHACRYLATE (PMMA) FOR 75 MINUTES WITH WATER, HAVING AN AVERAGE VALUE OF 32.55°

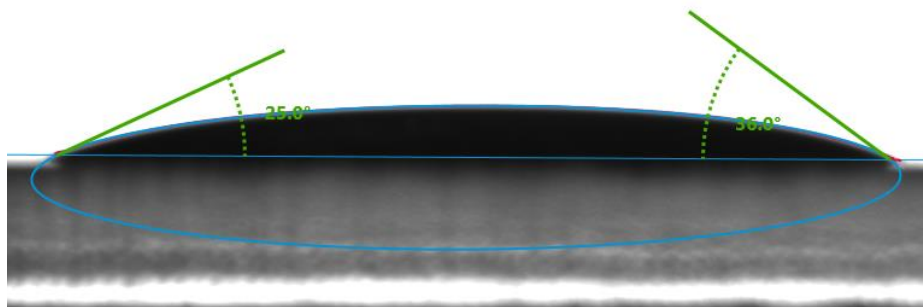


FIGURE 37 VALUE OF CONTACT ANGLE OF TREATED POLYMETHYL METHACRYLATE (PMMA) FOR 75 MINUTES WITH ETHYLENE GLYCOL, HAVING AN AVERAGE VALUE OF 30.5°

After performing Ozone Treatment for 90 Minutes:

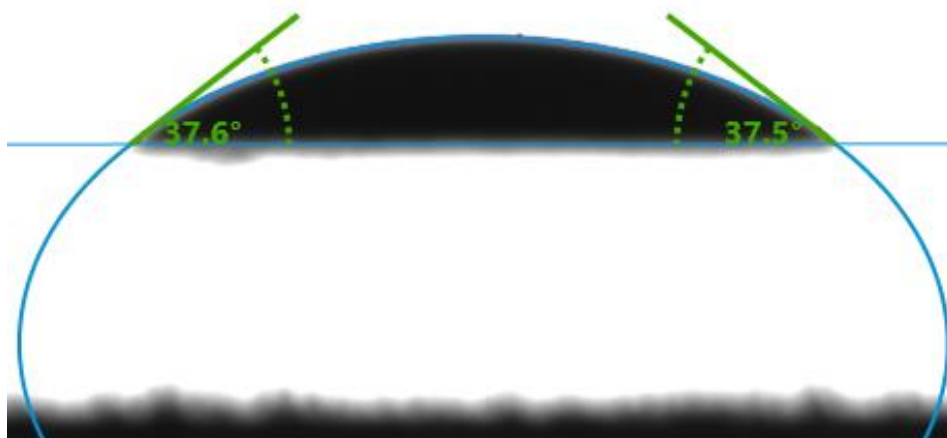


FIGURE 38 VALUE OF CONTACT ANGLE OF TREATED POLYMETHYL METHACRYLATE (PMMA) FOR 90 MINUTES WITH WATER, HAVING AN AVERAGE VALUE OF 37.55°

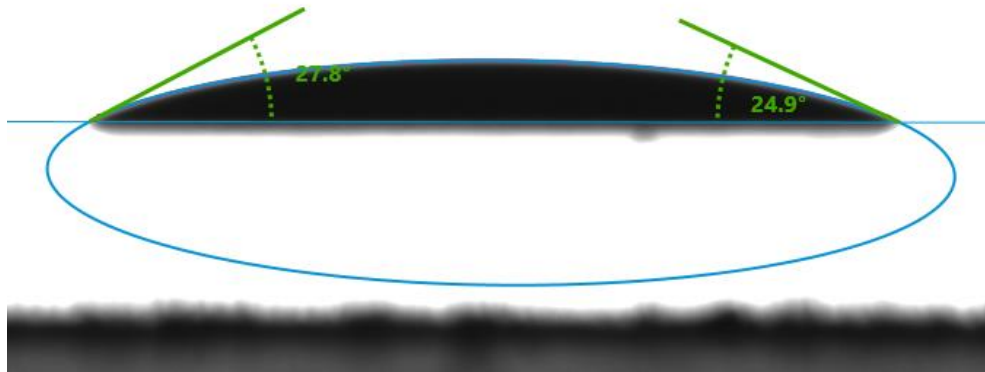


FIGURE 39 VALUE OF CONTACT ANGLE OF TREATED POLYMETHYL METHACRYLATE (PMMA) FOR 90 MINUTES WITH ETHYLENE GLYCOL, HAVING AN AVERAGE VALUE OF 26.35°

ANALYSIS

Ethylene Glycol led to better wettability as compared to water as oil wetted particles demonstrated a stronger tendency to float as compared to water wet particles. The more the oil particles float, it indicates enhanced wettability, meaning they will spread more effectively on the surface. [6]

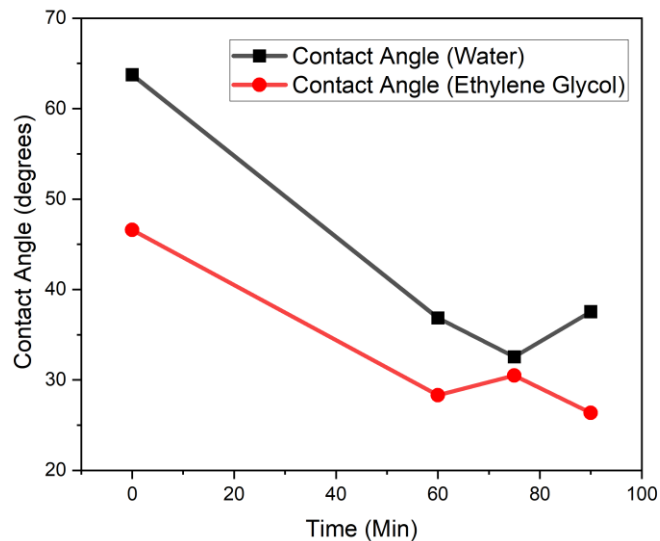


FIGURE 40 COMPARISON GRAPH OF VALUE OF CONTACT ANGLE ACHIEVED BY USING WATER AND ETHYLENE GLYCOL AS WETTING SOLVENTS

4.3.3 Surface Energies

Surface energies were calculated using water and ethylene glycol. The most relevant method is by contact angle measurements, which we used. It is the sum of dispersive and polar components of each liquid, respectively.

Table 4
Surface tension components of wetting solvents.

Wetting solvents	Polar component (mJ/m ²)	Dispersive component (mJ/m ²)	Surface free energy (mJ/m ²)
Water	51.0	21.8	72.8
Ethylene glycol	19.0	29.3	48.3

$$\gamma_L(1 + \cos \theta) = 2\sqrt{\gamma_S^d \gamma_L^d} + 2\sqrt{\gamma_S^p \gamma_L^p}$$

$$\gamma_S = \gamma_S^p + \gamma_S^d$$

FIGURE 41 VALUES AND EQUATIONS FOR CALCULATION OF SURFACE ENERGIES

4.3.3.1 Calculation of Surface Energies

According to the calculations made shown in **Error! Reference source not found.**, it is evident that as the value of contact angle was lowered, surface energy increased, enhancing the phenomena of wettability or ability of liquid to spread on a solid surface.

TABLE 5: CALCULATION OF SURFACE FREE ENERGIES

Conditions	Wetting Solvents	Polar Component (mJ/m ²)	Dispersive Component (mJ/m ²)	Surface Free Energy (mJ/m ²)
Without Ozone Treatment	Water Ethylene Glycol	41.3	29.9	71.2
Ozone Treatment for 15 Minutes	Water Ethylene Glycol	70.8	31.2	102.0
Ozone Treatment for 30 Minutes	Water Ethylene Glycol	79.8	25.1	104.9

Ozone Treatment for 45 Minutes	Water Ethylene Glycol	77.3	25.1	104.9
Ozone Treatment for 60 Minutes	Water Ethylene Glycol	74.9	21.8	96.7
Ozone Treatment for 75 Minutes	Water Ethylene Glycol	81.3	16.3	97.6
Ozone Treatment for 90 Minutes	Water Ethylene Glycol	73.2	24.1	97.3

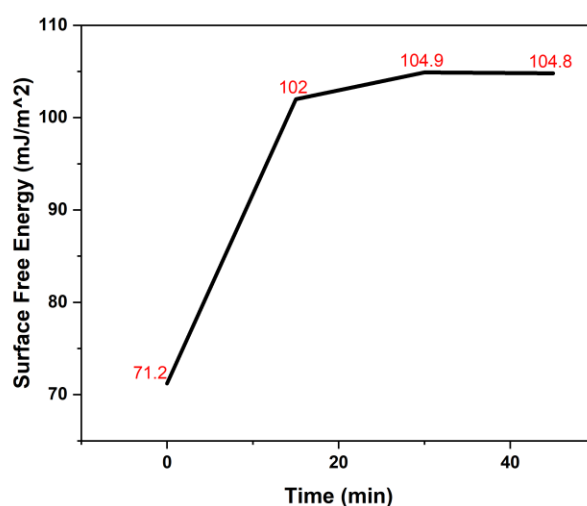


FIGURE 42 SURFACE FREE ENERGY VS TIME GRAPH FOR UNTREATED AND OZONE TREATED SAMPLES AT 15, 30 AND 45 MINUTES

4.3.4 UV-Vis Spectroscopy

The value of transmittance increased as ozone treatment was performed for longer time periods as the surface was cleaner and lesser contaminants were present. However, after 45 minutes, value of transmittance started to decrease. The reason related to this is the creation of various functional groups and pits on the surfaces. Value of more than 90% was achieved in all cases, making us reach our main objective.

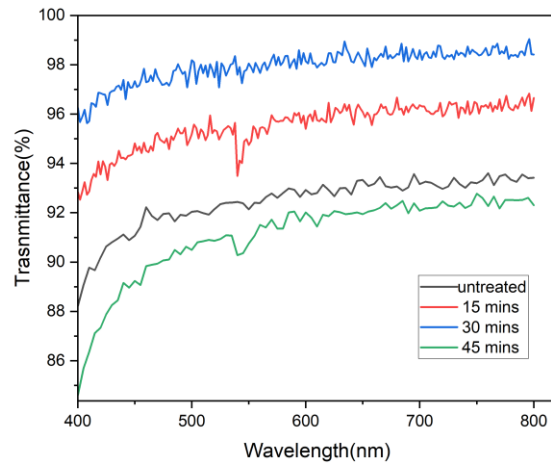


FIGURE 43 COMPARISON GRAPH OF UV-VIS SPECTROSCOPY RESULTS WITH SURFACE PRE-TREATMENT OF DIFFERENT INTERVALS

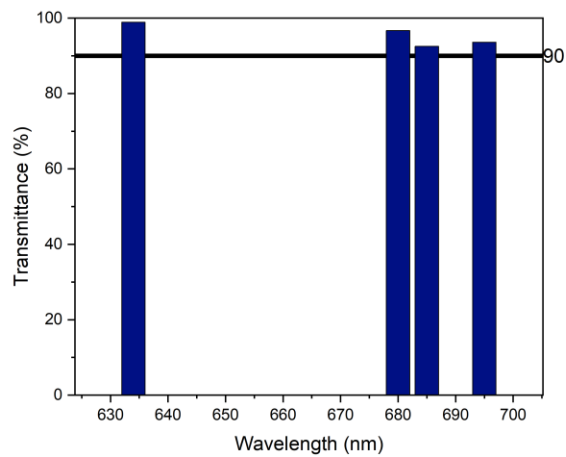


FIGURE 44 BAR GRAPH SHOWING MAXIMUM VALUES OF TRANSMITTANCE ACHIEVED

After checking the transmittances, surface pre-treated samples were acquired for lamination:

4.3.4.1 Sample 1

- Temperature: 105 °C
- Pressure
- MPa

- Time: 2 hrs.
- Layers: 1

The sample underwent a thorough cleaning procedure using a mixture of ethanol and lukewarm water in a 1:1 ratio. In the case of the initial sample, a total of 10 layers of polyurethane were applied. Examination of the accompanying figure reveals noticeable ripples and instances of delamination in the polyurethane, which can be attributed to the application of insufficient pressure during the lamination process.

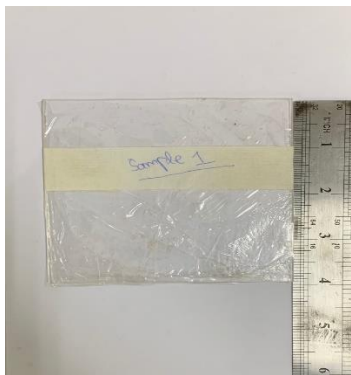


FIGURE 45 SAMPLE 1

4.3.4.2 Sample 2

- Temperature: 105 °C
- Pressure: 1 MPa
- Time: 3 hrs
- Layers: 10

After undergoing a meticulous cleaning process involving a 1:1 mixture of ethanol and lukewarm water, the initial sample received an application of 10 layers of polyurethane. Analysis of the corresponding figure brought to light evident ripples and instances of polyurethane delamination, attributable to the previous application of inadequate pressure during the lamination process. Notably, in subsequent attempts, the pressure was augmented to 1 MPa, resulting in a markedly improved lamination quality.

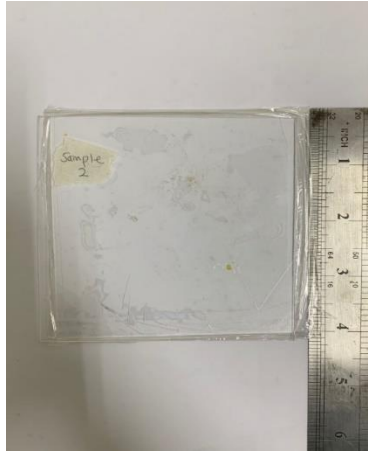


FIGURE 46 SAMPLE 2

4.3.4.3 Sample 3

- Temperature: Room Temperature
- Weight: 10 Kg
- Time: 24 hrs
- Adhesive Bonded with Polyurethane Film

Sample 3 was made using polyurethane adhesive. The adhesion mechanism between polyurethane adhesive and PMMA involves a multifaceted process. Initially, thorough surface preparation is essential, ensuring the removal of contaminants. The polyurethane adhesive forms chemical bonds with PMMA through reactive functional groups, and subsequent polymerization leads to the creation of a strong, cross-linked network. Additionally, molecular diffusion into the PMMA surface occurs during the curing process, further enhancing the interfacial bond. Mechanical interlocking contributes to adhesion by engaging with surface irregularities. Overall, the versatile bonding properties of polyurethane adhesive with PMMA are a result of a combination of chemical reactivity, curing mechanisms, and mechanical interlocking.

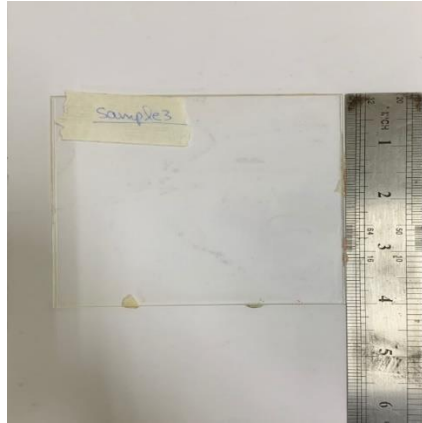


FIGURE 47 SAMPLE 3

4.3.4.4 Sample 4

- Temperature: Room Temperature
- Weight: 10 Kg
- Time: 24 hrs
- Adhesive Bonded with Polyurethane film

Sample 4 was constructed using both polyurethane film and polyurethane adhesive. However, the integration of these materials resulted in the formation of numerous voids and ripples. This outcome can be attributed to the inability of the polyurethane film to establish a cohesive interface with the polyurethane adhesive during the lamination process. The lack of effective bonding between the film and the adhesive led to the creation of undesirable imperfections, compromising the overall quality and structural integrity of the sample. [7]

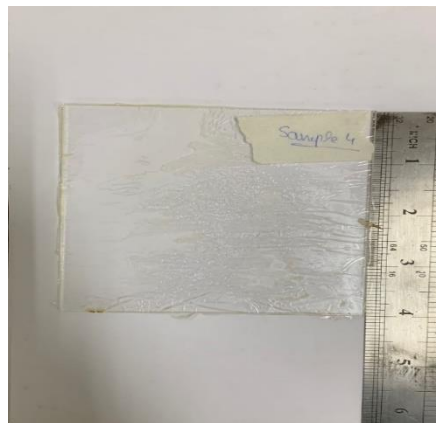


FIGURE 48 SAMPLE 4

4.3.5 PMMA Tensile test

4.3.6 Non-Laminated Sample

It shows the behavior of a material under tensile stress. Tensile stress is a pulling force that stretches the material. The experiment measures how much the material elongates (strain) under increasing amounts of stress. The strength of non-laminated sample came out to be 38 N/mm².

In Figure 30, the y-axis of the graph shows the stress placed on the material in megapascals (MPa). The x-axis shows the strain (percent elongation) as a percentage of the original length.

The graph can be divided into three regions. At the beginning of the curve, the stress and strain are proportional. This is the linear elastic region. In this region, the material deforms elastically, meaning it will return to its original shape once the stress is removed. The point at which the curve deviates from linearity is the yield point. This is the point at which the material begins to deform plastically. Plastic deformation is permanent. Once the stress is removed, the material will not return to its original shape. After the yield point, the material enters a region of strain hardening. In this region, the stress required to continue elongating the material increases. This is because the deformation of the material is making it stronger. Eventually, the material reaches a point where it can no longer withstand the stress and it necks down. Necking is a localized narrowing of the width of the sample. Once necking begins, the stress will rapidly decrease until the material fractures.

The stress-strain curve can be used to determine a number of important mechanical properties of a material, included in table 6:

TABLE 6: PROPERTIES DEFINITION

Property	
Young's modulus	This is a measure of the stiffness of the material. It is calculated by the slope of the linear elastic region of the curve.
Yield strength	This is the stress at the yield point
Ultimate tensile strength	This is the maximum stress that the material can withstand before it fractures.

Strain at break

This is the amount of strain that the material can withstand before it fractures.

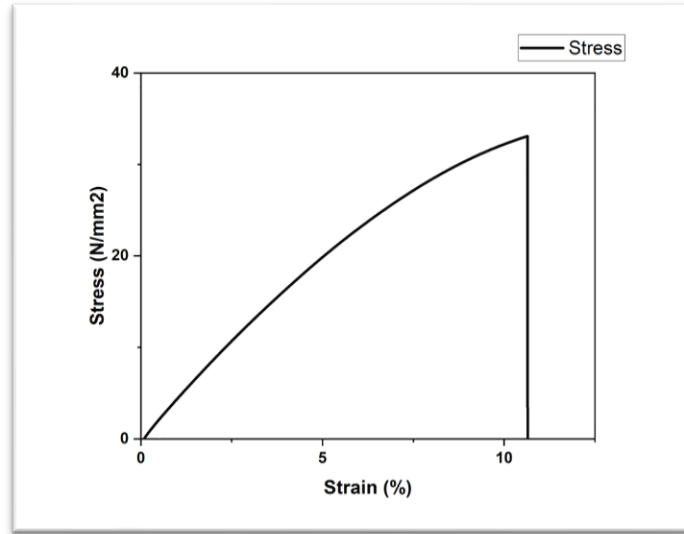


FIGURE 49 STRESS STRAIN GRAPH OF NON-LAMINATED SAMPLE

4.3.6.1 Sample 1

- Temperature: Room Temperature
- Weight: 10 Kg
- Time: 24 hrs
- Adhesive Bonded

In the initial graph, a gradual increase in stress is observed, reaching up to 36 MPa. Subsequently, the sample 1 graph reveals a significant increase in tensile strength, escalating from 36 MPa to 58 MPa. This notable increase is associated by varying parameters employed during the lamination process that is a temperature of 25°C, a load of 10 kg for 24 hours, and the use of a adhesive layer of polyurethane. Notably, the laminated PMMA sample exhibited a brittle fracture pattern as always, indicative of sudden and catastrophic failure under applied stress; However at higher values of stress.

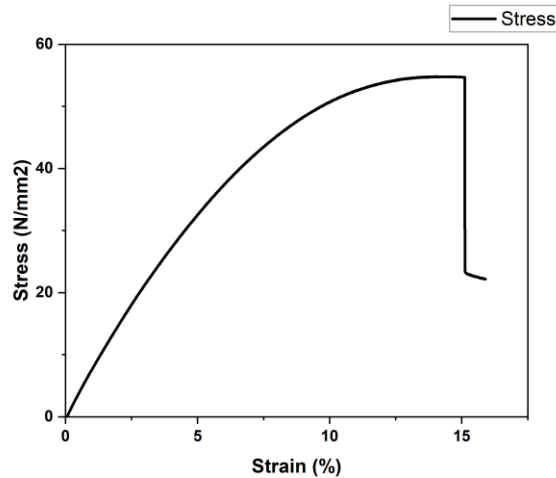


FIGURE 50 STRESS-STRAIN GRAPH OF SAMPLE 1

4.3.6.2 Sample 2

- Temperature: 105 °C
- Pressure: 1 MPa
- Time: 3 hours
- Layers: 1

Sample 2 underwent a lamination process under specific conditions, involving a temperature of 105 °C, a pressure of 1 MPa, and a duration of 3 hours. Additionally, a single layer of polyurethane was employed. Following this lamination, the sample was subjected to a tensile test using a testing machine. The results indicated that under these specified parameters, the sample exhibited the highest tensile strength, showcasing the effectiveness of the lamination process in enhancing the mechanical properties of the material.

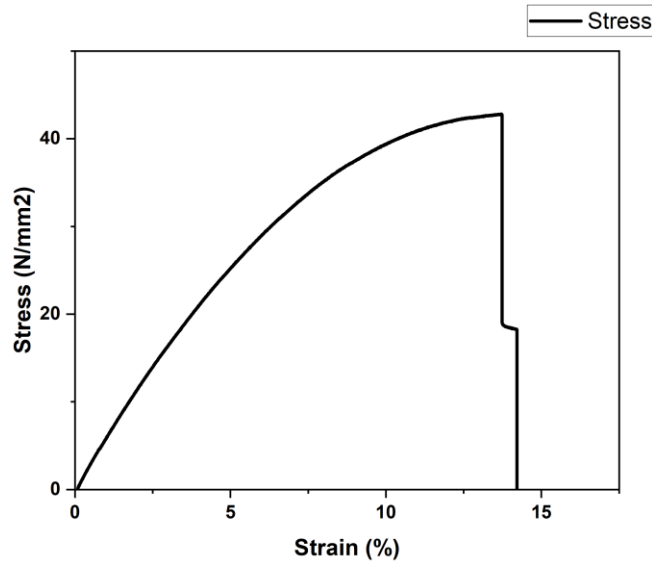


FIGURE 51 STRESS-STRAIN GRAPH OF SAMPLE 2

4.3.6.3 Sample 3

- Temperature: 105 °C
- Pressure: 1 MPa
- Time: 2 hours
- Layers: 1

In the case of Sample 3, a reduction in tensile strength is evident, declining to 43 MPa. This decrease can be attributed to the insufficient strength of the interlayer bond, the reason is that the polyurethane is unable to hold PMMA samples together due to lack of adhesive forces. The lack of adhesive forces and failure in Sample 3 can be attributed to potential incompatibility between the polyurethane and PMMA, resulting in poor interfacial bonding. This might be due to inadequate surface preparation, insufficient curing time, or inherent chemical incompatibility between the two materials, preventing the formation of strong adhesive bonds. Consequently, this leads to reduced tensile strength and the observed stepwise fracture pattern..

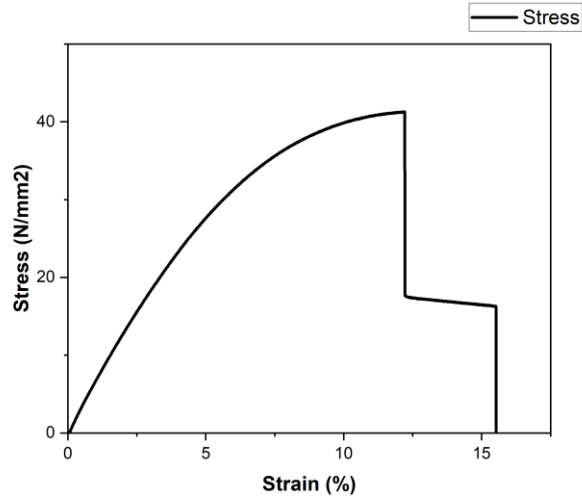


FIGURE 52 STRESS-STRAIN GRAPH OF SAMPLE 3

4.3.6.4 Sample 4

- Temperature: Room Temperature
- Weight: 10 Kg
- Time: 24 hrs
- Adhesive Bonded with Polyurethane film

Sample 4 exhibits a significant reduction in tensile strength, which drops to 39 MPa. The reason for this decrease is that the two laminated PMMA samples were not sufficiently secured due to a weak adhesive bond with the polyurethane sheet. However, when the conditions were set to room temperature, 10 kg of weight, and 24 hours of bonding time, the adhesive that was adhered to the polyurethane film showed diminished bonding. This

insufficiency is shown by a unique step in the graph that shows the breakage of one PMMA layer, which is followed by the breakage of the other PMMA layer.

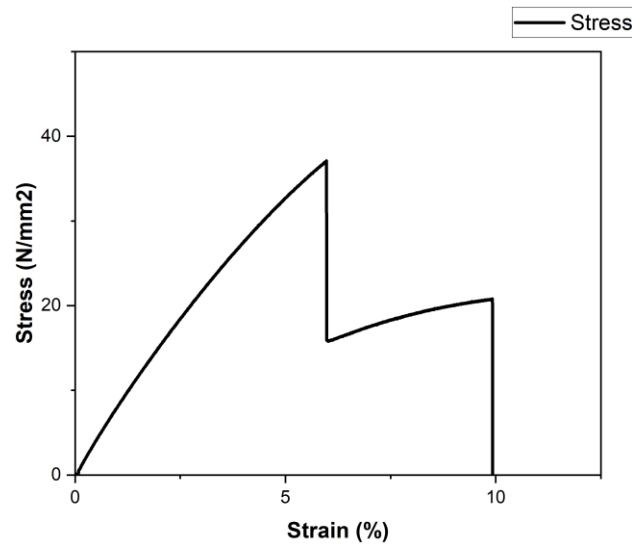


FIGURE 53 STRESS-STRAIN GRAPH OF SAMPLE 4

4.3.6.5 Sample 5

- Temperature: 90 °C
- Pressure: 1 MPa
- Time: 2 hours
- Layers: 1

The yield point is the point on the curve where the material begins to deform plastically. After the yield point, the stress increases more rapidly as the material deforms more. Eventually, the material will break. The breaking point is not shown in this graph.

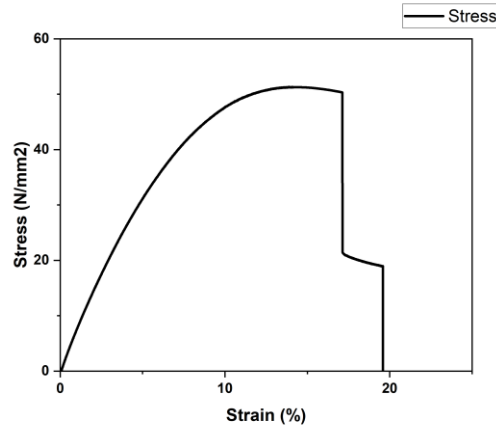


FIGURE 54 STRESS STRAIN GRAPH OF SAMPLE 5

4.3.6.6 Comparison

To provide an objective comparison of the tensile strength and stress-strain behavior of the different PMMA samples under various conditions, we can draw a table summarizing the key details for each sample. Here is the comparison:

TABLE 7 COMPARISON OF TENSILE STRENGTH AND STRESS-STRAIN BEHAVIOR OF PMMA SAMPLES

Sample	Conditions	Maximum Tensile Strength (MPa)	Observations	Fracture Pattern
Non-Laminated	-	38	Typical stress-strain behavior with elastic, plastic deformation, strain hardening, and necking regions	Brittle fracture at higher stress
Sample 1	Room Temperature, 10 kg weight, 24 hrs, Adhesive Bonded	58	Significant increase in tensile strength due to effective lamination; notable increase from 36 MPa to 58 MPa	Brittle fracture at higher stress
Sample 2	105 °C, 1 MPa, 3 hours, 1 Layer	Highest (exact value not provided)	Highest tensile strength observed; effective lamination enhances mechanical properties	Not specified
Sample 3	105 °C, 1 MPa, 2 hours, 1 Layer	43	Reduction in tensile strength due to insufficient interlayer bond strength; step in graph indicates sequential layer fracture	Not specified

Sample 4	Room Temperature, 10 kg weight, 24 hrs, Adhesive Bonded with Polyurethane Film	39	Significant reduction in tensile strength; weak adhesive bond leading to unique step indicating sequential layer fracture	Not specified
Sample 5	90 °C, 1 MPa, 2 hours, 1 Layer	Not specified	Standard stress-strain behavior until yield point; stress increases more rapidly post-yield	Not shown

4.3.7 Summary of Key Observations

4.3.8 Non-Laminated Sample

Exhibits typical stress-strain behavior with regions of elastic deformation, plastic deformation, and strain hardening.

Maximum tensile strength: 38 MPa.

Brittle fracture pattern observed at higher stress values.

4.3.8.1 Sample 1

Lamination process at room temperature with 10 kg weight for 24 hours using adhesive.

Significant increase in tensile strength to 58 MPa.

Brittle fracture pattern under higher stress values.

4.3.8.2 Sample 2

Lamination at 105 °C, 1 MPa pressure, for 3 hours with a single layer.

Exhibits the highest tensile strength, indicating the effectiveness of lamination.

Exact maximum tensile strength not provided.

4.3.8.3 Sample 3

Lamination at 105 °C, 1 MPa pressure, for 2 hours with a single layer.

Reduced tensile strength to 43 MPa due to insufficient interlayer bond strength.

Unique step in the stress-strain graph indicates sequential layer fracture.

4.3.8.4 Sample 4

Lamination at room temperature with 10 kg weight for 24 hours using polyurethane film.

Reduced tensile strength to 39 MPa due to weak adhesive bond.

Unique step in the stress-strain graph indicates sequential layer fracture.

4.3.8.5 Sample 5

Lamination at 90 °C, 1 MPa pressure, for 2 hours with a single layer.

Standard stress-strain behavior with linear increase until the yield point.

Post-yield behavior not fully detailed, but the breaking point is not shown.

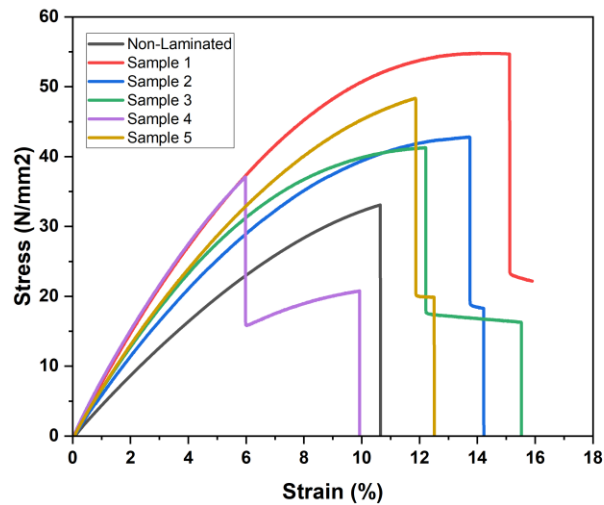


FIGURE 55 TENSILE TEST GRAPH OVERLAPPING FOR COMPARISON

CONCLUSION

It can be concluded that the project was completed successfully, achieving our desired results. The ideal timing for surface pre-treatment was 30 minutes, followed by a lamination value of 96% and the highest tensile strength achieved was 61.1 N/mm^2 . This process can be effectively implemented in the canopy of the Hurkus-C aircraft, owned by Turkish Aerospace Industries (TAI), ensuring the pilot has a clear view while also providing protection from external elements, including bird strikes. Currently, the Aircraft Rebuild Factory (ARF) at Pakistan Aeronautical Complex (PAC), Kamra, manufactures monolithic canopies using Polymethyl methacrylate (PMMA) alone, which exhibit poor impact toughness. Our final year design project (FYDP) focused on enhancing this by bonding two sheets of PMMA using Polyurethane (PU) as an adhesive. The sheets were heated above PU's melting point in a hot press, forming a robust bond that improved the canopy's impact toughness without compromising its optical transparency. Optical transparencies, which allow light to easily pass through, are critical for various applications, including lenses, optics, windows, photovoltaic devices, displays, and screens. In our study, the laminated canopy demonstrated optical transparency exceeding 95%. We confirmed the smooth surface morphology of the material using Scanning Electron Microscopy (SEM) and analyzed the surface chemistry with Fourier Transform Infrared Spectroscopy (FTIR), identifying the chemical bonds in PMMA and PU. In the future, we plan to explore advanced lamination techniques using materials like polycarbonate to further enhance the performance of the canopy.

REFERENCES

1. Baldan, A. (2012). Adhesion phenomena in bonded joints. *International Journal of Adhesion and Adhesives*, 38, 95–116. <https://doi.org/10.1016/j.ijadhadh.2012.04.007>
2. Armistead, S. (2017). DSIAC TECHNICAL INQUIRY (TI) RESPONSE REPORT Department of Defense (DoD) and Commercial Aircraft Transparency Construction, Materials, and Applications REPORT PREPARED BY. www.DSIAC.org.
3. Neto, M. D. B., Sales, R. D. C. M., Koshun, I., & Rocco, J. A. F. F. (2016). Reinforced transparencies for aerospace application – case description. *Journal of Aerospace Technology and Management*, 8(1), 49–54. <https://doi.org/10.5028/jatm.v8i1.575>
4. Dong, L., Li, Y., Huang, M., Hu, X., Qu, Z., & Lu, Y. (2022). Effect of anodizing surface morphology on the adhesion performance of 6061 aluminum alloy. *International Journal of Adhesion and Adhesives*, 113. <https://doi.org/10.1016/j.ijadhadh.2021.103065>
5. Altay, B. N., Fleming, P. D., Rahman, M. A., Pekarovicova, A., Myers, B., Aydemir, C., & Karademir, A. (2022). Controlling unequal surface energy results caused by test liquids: the case of UV/O3 Treated PET. *Scientific Reports*, 12(1). <https://doi.org/10.1038/s41598-022-10816-6>
6. Ardila-Rodríguez, L. A., Boshuizen, B., Rans, C., & Poulis, J. A. (2021). The influence of grit blasting and UV/Ozone treatments on Ti-Ti adhesive bonds and their durability after sol-gel and primer application. *International Journal of Adhesion and Adhesives*, 104. <https://doi.org/10.1016/j.ijadhadh.2020.102750>
7. "Martín, M., et al., Polymeric interlayer materials for laminated glass: A review. *Construction and Building Materials*, 2020. 230: p. 116897.," [Online].
8. Wouters, J. M., & Doe, P. J. (1991). Acrylic mechanical bond tests (No. LA-SUB-93-213-1). Los Alamos National Lab.(LANL), Los Alamos, NM (United States).
9. Read, C. J. (2004). Standard test method for bird impact testing of aerospace transparent enclosures. *ASTM F330-89*, 8.
10. Askari, A., Nelson, K., Weckner, O., Xu, J., & Silling, S. (2011). Hail impact characteristics of a hybrid material by advanced analysis techniques and testing. *Journal of Aerospace Engineering*, 24(2), 210-217.
11. Standard, A. S. T. M. (2010). D638: Standard test method for tensile properties of plastics. *West Conshohocken (PA): ASTM International*.

12. Thackeray, K., & Hinkley, J. (2022). Mechanical Testing and Properties of Plastics—An Introduction.
13. Stenzler, J. S., & Goulbourne, N. C. (2011, April). Effect of Polyacrylate Interlayer microstructure on the impact response of multi-layered polymers. In *Time Dependent Constitutive Behavior and Fracture/Failure Processes, Volume 3: Proceedings of the 2010 Annual Conference on Experimental and Applied Mechanics* (pp. 241-258). New York, NY: Springer New York.
14. Wang, X. K., Wei, S. C., Xu, B. S., Chen, Y., Yan, X., & Xia, H. H. (2015). Transparent organic materials of aircraft cockpit canopies: research status and development trends. *Materials Research Innovations*, 19(sup10), S10-199.
15. Fischer, W. F., LeMasters, D. P., & Harbison, W. C. (1986). *U.S. Patent No. 4,594,290*. Washington, DC: U.S. Patent and Trademark Office.
16. Galeotti, F., Mróz, W., Catellani, M., Kutrzeba-Kotowska, B., & Kozma, E. (2016). Tailorable perylene-loaded fluorescent nanostructures: a multifaceted approach enabling application in white hybrid LEDs. *Journal of Materials Chemistry C*, 10, C6TC00486E.
17. ASTM, D. (2021). 1003: Standard Test Method for Haze and Luminous Transmittance of Transparent Plastics. *ASTM International*.
18. ASTM, D. (1995). Standard test method for yellowness index of plastics. *American Society for Testing and Materials, Philadelphia*.
19. WISER, G. L. (1971). Transparency applications of polycarbonates. *Aircraft Engineering and Aerospace Technology*, 43(8), 18-20.
20. Huyett, R. A., Wintermute, G. E., & GOODYEAR AEROSPACE CORP LITCHFIELD PARK AZ. (1976). *Environmental Resistance of Coated and Laminated Polycarbonate Transparencies*. NTIS.
21. Golden, J. H., Hammant, B. L., & Hazell, E. A. (1968). Effects of molecular weight and strain rate on the flexural properties of polycarbonate. *Journal of Applied Polymer Science*, 12(3), 557-569.
22. Rühl, A., Kolling, S., & Schneider, J. (2017). Characterization and modeling of poly (methyl methacrylate) and thermoplastic polyurethane for the application in laminated setups. *Mechanics of Materials*, 113, 102-111.

23. Axilrod, B. M., Sherman, M. A., Cohen, V., & Wolock, I. (1952). *Effects of moderate biaxial stretch-forming on tensile and crazing properties of acrylic plastic glazing* (No. NACA-TN-2779).
24. Hedayati, R., Ziaei-Rad, S., Eyvazian, A., & Hamouda, A. M. (2014). Bird strike analysis on a typical helicopter windshield with different lay-ups. *Journal of Mechanical Science and Technology, 28*, 1381-1392.
25. Clayton, K. I., Milholland, J. F., & Stenger, G. J. (1981). Experimental Evaluation of F-16 Polycarbonate Canopy Material. *University of Daytona Research Institute, AFWAL-TR-81, 4020*, 129.
26. Clayton, K. I., West, B. S., Bowman, D. R., & DAYTON UNIV OH RESEARCH INST. (1986). *Aircraft Transparency Test Methodology* (p. 0190). AFWAL-TR-85-3125, March.
27. Schwartz, J. J., Chuang, H. J., Rosenberger, M. R., Sivaram, S. V., McCreary, K. M., Jonker, B. T., & Centrone, A. (2019). Chemical identification of interlayer contaminants within van der Waals heterostructures. *ACS applied materials & interfaces, 11*(28), 25578-25585.
28. Stenzler, J. S. (2009). *Impact mechanics of PMMA/PC multi-laminates with soft polymer interlayers* (Doctoral dissertation, Virginia Tech).
29. Bos, F. P., Veer, F. A., Belis, J., Louter, P. C., & Nieuwenhuijzen, E. V. (2005). The joints of the All Transparent Pavilion. *Proceedings 9th Glass Processing Days, Tampere, Finland*.
30. Larson, K. (1991). *Improved Optical Interlayer Systems Show Bond Stability at High Temperatures, High Humidity* (No. 911136). SAE Technical Paper.
31. Bouchard, M. P., Bowman, D. R., & Whitney, T. J. (1999, January). Aging of Aircraft Transparencies. In *NASA Conference Publication* (pp. 91-100). NASA.
32. Folgar, F. (2005). Advanced aliphatic polyurethane resins for high durability and superior ballistic performance laminated glass. In *22nd International symposium on ballistics. Vancouver BC, Canada: DEStech Publications, Inc* (pp. 908-16).
33. Fountzoulas, C. G., Cheeseman, B. A., Dehmer, P. G., & Sands, J. M. (2007). *A computational study of laminate transparent armor impacted by FSP*. Army Research Laboratory.
34. Stenzler, J. S., & Goulbourne, N. (2009, June). Impact mechanics of transparent multi-layered polymer composites. In *Proceedings of the Society for Experimental Mechanics-Sem Annual Conference and Exposition on Experimental and Applied Mechanics*.